



HAL
open science

A model for establishment, maintenance and reactivation of the immune response after vaccination against Ebola virus

Irene Balelli, Chloé Pasin, Mélanie Prague, Fabien Crauste, Thierry van Effelterre, Viki Bockstal, Laura Solforosi, Rodolphe Thiébaud

► **To cite this version:**

Irene Balelli, Chloé Pasin, Mélanie Prague, Fabien Crauste, Thierry van Effelterre, et al.. A model for establishment, maintenance and reactivation of the immune response after vaccination against Ebola virus. *Journal of Theoretical Biology*, 2020, 495, pp.110254. 10.1016/j.jtbi.2020.110254 . hal-03160892v2

HAL Id: hal-03160892

<https://hal.science/hal-03160892v2>

Submitted on 24 Jun 2020

HAL is a multi-disciplinary open access archive for the deposit and dissemination of scientific research documents, whether they are published or not. The documents may come from teaching and research institutions in France or abroad, or from public or private research centers.

L'archive ouverte pluridisciplinaire **HAL**, est destinée au dépôt et à la diffusion de documents scientifiques de niveau recherche, publiés ou non, émanant des établissements d'enseignement et de recherche français ou étrangers, des laboratoires publics ou privés.

A model for establishment, maintenance and reactivation of the immune response after vaccination against Ebola virus

Irene Balelli^{a,b,c,*}, Chloé Pasin^{a,b,c,d}, Mélanie Prague^{a,b,c}, Fabien Crauste^e,
Thierry Van Effelterre^f, Viki Bockstal^g, Laura Solforosi^g, Rodolphe
Thiébaud^{a,b,c}

^a*INSERM U1219 Bordeaux Population Health, Université de Bordeaux, Bordeaux, France*

^b*INRIA SISTM team, Talence, France*

^c*Vaccine Research Institute, Créteil, France*

^d*Department of Pathology and Cell Biology, Columbia University Medical Center, New York, New York, USA*

^e*Université de Bordeaux, CNRS, Bordeaux INP, IMB, UMR 5251, F-33400 Talence, France*

^f*Janssen Pharmaceutica N.V., Beerse, Belgium*

^g*Janssen Vaccines & Prevention B.V., Leiden, The Netherlands*

Abstract

The 2014-2016 Ebola outbreak in West Africa has triggered accelerated development of several preventive vaccines against Ebola virus. Under the EBO-VAC1 consortium, three phase I studies were carried out to assess safety and immunogenicity of a two-dose heterologous vaccination regimen developed by Janssen Vaccines and Prevention in collaboration with Bavarian Nordic. To describe the immune responses induced by the two-dose heterologous vaccine regimen, we propose a mechanistic ODE based model, which takes into account the role of immunological memory. We perform identifiability and sensitivity analysis of the proposed model to establish which kind of biolog-

*Corresponding author

Email addresses: irene.balelli@u-bordeaux.fr (Irene Balelli),
cgp2121@cumc.columbia.edu (Chloé Pasin), melanie.prague@u-bordeaux.fr (Mélanie Prague),
fabien.crauste@u-bordeaux.fr (Fabien Crauste), tvaneffe@ITS.JNJ.com (Thierry Van Effelterre),
vbocksta@its.jnj.com (Viki Bockstal),
lsolforo@its.jnj.com (Laura Solforosi), rodolphe.thiebaut@u-bordeaux.fr (Rodolphe Thiébaud)

ical data are ideally needed in order to accurately estimate parameters, and additionally, which of those are non-identifiable based on the available data. Antibody concentrations data from phase I studies have been used to calibrate the model and show its ability in reproducing the observed antibody dynamics. Together with other factors, the establishment of an effective and reactive immunological memory is of pivotal importance for several prophylactic vaccines. We show that introducing a memory compartment in our calibrated model allows to evaluate the magnitude of the immune response induced by a booster dose and its long-term persistence afterwards.

Keywords: Mechanistic modeling, Immunological memory, Vaccination, Ebola Virus, Identifiability analysis, Sensitivity analysis, Calibration, Heterologous vaccination

1. Introduction

Since the discovery of Ebola virus in 1976, recurring Ebola outbreaks have been recorded in equatorial Africa [1, 2]. The largest outbreak ever recorded has affected West Africa between March 2014 and June 2016 [3], during which a Public Health Emergency of International Concern was declared, and resulted in more than 28,000 cases and 11,000 deaths, since no licensed vaccines nor cure were available. On August 1st 2018 a new Ebola outbreak was declared in the Democratic Republic of Congo (DRC) in North Kivu and Ituri provinces [4]. At present, it has been confined to a relatively small area but has already caused more than 3400 confirmed cases and 2250 confirmed deaths updated to March 1st 2020 [5]: the World Health Organization (WHO) declared a Public Health Emergency of International Concern on July 17th 2019 [6].

Ebola virus (EBOV) belongs to the Filoviridae family, which includes five well-known species (Zaire (ZEBOV), Bundibugyo, Sudan, Reston and Tai Forest), and the recently discovered Bombali species [7]. Ebola virus causes Ebola Viral Disease (EVD), a severe and acute illness, with a mortality rate ranging from 25% to 90% according to the WHO [2]. Therefore, there is an urgent need for licensed Ebola vaccines.

In response to the 2014-2016 Ebola outbreak, the development of several vaccine candidates against Ebola virus has been accelerated, with various

24 vaccine platforms and antigen inserts [8, 9]. In this context, in December
25 2014 the EBOVAC1 consortium was built under the Innovative Medicines
26 Initiative Ebola+ Program. Its purpose was to support the development by
27 Janssen Vaccines & Prevention B.V. of a new two-dose heterologous vaccine
28 regimen against Ebola based on Adenovirus serotype 26 (Ad26.ZEBOV) and
29 Modified Vaccinia Ankara (MVA-BN-Filo) vectors [10]. Ad26.ZEBOV vector
30 encodes the glycoprotein (GP) of the Ebola Zaire virus, while MVA-BN-Filo
31 encodes GPs from Ebola Zaire virus, Ebola Sudan virus, Marburg virus, and
32 Tai Forest virus nucleoprotein.

33
34 The proposed two-dose regimens utilize both vaccines, administered at
35 28 or 56 days intervals. Three phase I studies have been carried out in four
36 countries under EBOVAC1: United Kingdom [11, 12], Kenya [13], Uganda
37 and Tanzania [14]. The immune response following vaccination has been
38 evaluated up to one year after the first dose through GP-specific binding an-
39 tibody concentrations. Neutralizing antibody and T cell responses have also
40 been evaluated up to one year of follow-up. Although human efficacy data
41 are not available, results on non-human primate models have shown that the
42 antibody concentration after the challenge correlates best with survival upon
43 intramuscular challenge with Ebola virus [15, 16, 17, 18].

44
45 Therefore, it becomes relevant to estimate the persistence of the anti-
46 body response induced by the two-dose heterologous vaccine. The *in silico*
47 approach we propose here will provide a good starting point to predict the
48 humoral immune response elicited by the proposed vaccination regimen be-
49 yond the available persistence immunogenicity data.

50
51 The goal of prophylactic vaccination is to induce immunity against an in-
52 fectious disease. Henceforth, it aims at stimulating the immune system and
53 its ability to store and recall information about a specific pathogen, leading to
54 a long-term protective immunity. This is possible by means of immunological
55 memory, one of the core features of adaptive immune responses [19, 20, 21].

56
57 By generating specific antibodies, B cells play a key role in the mam-
58 malian adaptive immune system, and help protecting the organism against
59 antigenic challenges. Several populations of specific B cells are generated
60 upon antigen stimulation, with distinct functional roles. Naïve B cells be-
61 come activated through the encounter with the antigen in secondary lym-

62 phoid organs. Upon activation, they can either become short-lived Antibody
63 Secreting Cells (ASCs), or seed highly dynamic environments called Ger-
64 minal Centers (GCs). In the second circumstance, B cells undergo B cell
65 receptor (BCR) affinity maturation to improve their affinity against the pre-
66 sented antigen. The interaction of B cells with follicular dendritic cells and
67 follicular helper T cells within GCs allows selection of B cells with improved
68 antigen-binding ability [22]. During the course of a GC reaction, B cells
69 can become either memory B cells or long-lived ASCs depending on the
70 strength of their affinity. In particular, long-lived ASCs are generated after
71 extensive B cells affinity maturation and produce high affinity antibodies. In
72 contrast, memory B cells undergo less extensive affinity maturation, making
73 them promptly available. Ultimately, ASCs are differentiated B cells able to
74 produce high-affinity antibodies [22, 23, 24].

75
76 The primary infection induces a transient antibody response, because it
77 is mostly characterized by short-lived ASCs. Indeed, findings on the kinetics
78 of circulating ASCs following vaccination show an early peak located around
79 7 days after vaccination, followed by a rapid relaxation phase: their level be-
80 comes undetectable after 10 to 14 days [25, 26, 27]. Nevertheless, the primary
81 infection is able to elicit memory B cells, which play a key role in protection
82 against subsequent infections with the same pathogen. Indeed, secondary
83 exposure to a priming antigen is characterized by a more rapid and intense
84 humoral response, which is of better quality as well (*i.e.* higher affinity an-
85 tibodies) [28, 29]: this is the so called anamnestic response. Memory B cells
86 can directly differentiate into short-lived ASCs, as well as seed new GCs for
87 further affinity maturation [22, 30]. This is done in a more effective way
88 than naïve B cells: it has been experimentally observed that memory B cells
89 possess an intrinsic advantage over naïve B cells in both the time to initiate
90 a response and in the division-based rate of effector cell development [29].
91 Once the infection has been controlled, the generated population of specific
92 B cells contracts, leaving memory B cells and long-lived ASCs. The latter
93 population partially migrates to the bone-marrow and assures long-term pro-
94 duction of high-affinity antibodies [31, 32].

95
96 Mathematical models of the immune response are increasingly recognized
97 as powerful tools to gain understanding of complex systems. Several math-
98 ematical models have already been developed to describe antibody decay
99 dynamics following vaccination or natural infection aiming at predicting long-

100 term immunity. The more popular models are simple exponential decay mod-
101 els (*e.g.* [33, 34]), bi-exponential decay models (*e.g.* [35, 36]) or power-law
102 decay models (*e.g.* [37]). They are based on the assumption that antibody
103 concentrations will decay over time. Changing slopes can be introduced to
104 better fit immunological data, which typically show a higher antibody decay
105 during the first period after immunization followed by a slower antibody de-
106 cay.

107

108 ODE-systems are an extremely useful tool to model complex systems,
109 because they are relatively easy to communicate, new biological assumptions
110 can be included and several softwares exist to compute numerical solutions.
111 To gain better insights on the dynamics of the humoral response, Le *et al.*
112 [38] proposed a model taking into account a population of specific ASCs and
113 applied it to fit data from both ASCs and antibodies upon vaccinia virus
114 immunization of human volunteers. This is the extension of a model devel-
115 oped by De Boer *et al.* [39] and Antia *et al.* [40] for modeling the CD8
116 T cell response. As stressed by the authors, this model may underestimate
117 long-term immunity since it does not take into consideration antibody con-
118 tribution supplied by long-lived ASCs [31, 32].

119

120 The assumption of having several ASCs populations has been considered
121 in several models thereafter. Fraser *et al.* [41] considered an extension of
122 the conventional power-law decay model to include two distinct populations
123 of ASCs, differing in they respective decay rate, showing an improvement
124 of data fitting. Andraud *et al.* and White *et al.* [42, 43] developed models
125 based on ordinary differential equations (ODEs) describing the contribution
126 of short and long-lived ASCs in antibody production.

127

128 All previously cited models focus on the humoral response following im-
129 munization, without questioning the ability of the immune system to mount
130 anamnestic responses. To the best of our knowledge, very few models have
131 been proposed to address this question. An example is given by Wilson and
132 Nokes [44, 45]. The authors explored different mechanisms for the genera-
133 tion of immune memory and its role in enhancing a secondary response upon
134 further immunization against hepatitis B virus. The memory compartment
135 included memory B and T cells and followed a logistic behavior. In this work,
136 antibody and memory cell generation depended on the circulating antigen.
137 The authors did not consider the contribution of any population of ASCs in

138 generating and sustaining the antibody response. A memory B cell compart-
139 ment, where memory B cells are supposed to follow a logistic behavior and
140 could differentiate into ASCs, has been considered by Davis *et al.* [46]. The
141 authors parametrized a model based on 12 ODEs of the humoral immune
142 response against Shigella, a diarrheal bacteria, to describe the complex in-
143 teractions of the bacteria with the host immune system. Nevertheless, the
144 complexity of the proposed model entails several identifiability issues, mak-
145 ing it difficult to be used in practice.

146
147 Pasin *et al.* [47] have already analyzed the antibody response elicited
148 by the two-dose heterologous vaccine regimens against Ebola virus based on
149 Ad26.ZEBOV and MVA-BN-Filo, and evaluated during three phase I stud-
150 ies under the EBOVAC1 project. To this extent, they have used the model
151 developed by Andraud *et al.* [42]. Model parameters have been estimated
152 using a population approach and some key factors inducing variability in the
153 humoral response have been identified and quantified. The model used by
154 Pasin *et al.* focuses on the antibody response observed after the second dose,
155 and can help predicting the durability of the antibody response following the
156 two-dose heterologous regimens. However, the anamnestic response of any
157 new exposure could not be studied, because no plasma cells nor memory B
158 cells generation mechanism has been considered.

159
160 Here we want to extend the model developed by Andraud *et al.* [42] to
161 characterize the establishment of the humoral response after the first vac-
162 cine dose and its reactivation following the second dose. The generation of
163 different subgroups of B cells -memory, short- and long-lived ASCs- is taken
164 into account and a vaccine antigen compartment is considered as responsible
165 for inducing the immune response. We aim at understanding the ability of
166 vaccinated people to react to a potential future encounter with Ebola virus
167 antigens. To this extent, we develop a model able to describe the generation
168 of an anamnestic response by means of the establishment of the immunolog-
169 ical memory.

170
171 Description of studies performed under the EBOVAC1 project and a de-
172 scriptive analysis of antibody concentrations are given in Section 2. In Sec-
173 tion 3 we formulate our mathematical model describing the humoral response
174 to a single immunization and explain how it can be used to simulate further
175 immunizations. In Section 4 we perform structural identifiability analysis to

176 determine which data should be generated or alternatively which parame-
177 ters should be fixed to allow proper parameter estimation. In Section 5 we
178 perform a model calibration against available antibody concentration mea-
179 surements. In Section 6, local sensitivity analysis completes previous results
180 on parameter identifiability. With the parameter set obtained through cal-
181 ibration, in Section 7 we simulate a booster immunization which shows an
182 improved immune response, due to the establishment of immunological mem-
183 ory elicited by the two-dose vaccination regimens. Finally in Section 8 we
184 discuss the significance of obtained results and limitations of the model.

185

186 2. Study design and serological analyses

187 We consider data collected during three randomized, blinded, placebo-
188 controlled phase I studies on healthy adult volunteers aged 18 to 50 years.
189 Studies were performed in four different countries: UK, Kenya, Uganda and
190 Tanzania. We present briefly these data here, because we will use them in
191 next sections (*e.g.* Section 5). We refer to [11, 12, 13, 14] for a detailed
192 presentation of safety and immunogenicity results, for studies in UK, Kenya
193 and Uganda/Tanzania respectively.

194

195 In each country, participants were randomized into four vaccination groups
196 differing by the order of vaccine immunizations (Ad26.ZEBOV as first dose
197 and MVA-BN-Filo as second dose or conversely) and by the interval of time
198 between immunizations (either 28 or 56 days). Throughout the paper we
199 will label vaccination groups specifying the order of vaccine immunizations
200 and delay between the first and second doses, *e.g.* participants within group
201 Ad26/MVA D57 have received the first Ad26.ZEBOV dose at day 1 and the
202 second MVA-BN-Filo dose 56 days later. Vaccination group Ad26/MVA D57
203 will be considered as the reference group. In each study 18 volunteers were
204 enrolled per vaccination group, 3 receiving placebo and 15 receiving active
205 vaccine.

206

207 We have analyzed data from a total of 177 participants subdivided as de-
208 scribed in Table 1. For all groups immunogenicity measurements have been
209 recorded at the first immunization day (day 1), 7 days later (day 8), at the
210 second immunization day (day 29 or 57), at both 7 days (day 36 or 64) and
211 21 days (day 50 or 78) after the second immunization, and at days 180, 240

Table 1: Summary of data analyzed per vaccination group.

Group	No.	Measurements
MVA/Ad26 D29	44	D1, D8, D29, D36, D50, D180, D240, D360
MVA/Ad26 D57	44	D1, D8, D29, D57, D64, D78, D180, D240, D360
Ad26/MVA D29	45	D1, D8, D29, D36, D50, D180, D240, D360
Ad26/MVA D57	44	D1, D8, D29, D57, D64, D78, D180, D240, D360
Total	177	

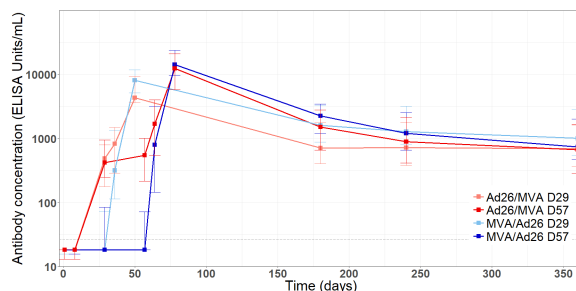


Figure 1: Antibody concentrations dynamics per vaccination group in \log_{10} scale.

212 and 360 after the first immunization for the follow-up. Groups receiving the
 213 second dose at day 57 have an extra immunogenicity measurement at day 29.

214

215 The humoral immune response to the vaccine has been assessed through
 216 analysis of IgG binding antibody concentrations against the Ebola virus Kik-
 217 wit variant glycoprotein (EBOV GP). This was determined by enzyme-linked
 218 immunosorbent assay (ELISA) performed by Battelle Biomedical Research
 219 Center (BBRC, US) for the UK and Uganda/Tanzania studies and by Q2 So-
 220 lutions (US) for the Kenya study with assay-specific limit of detection (LOD)
 221 varying among analyzing laboratory (36.6 ELISA units/mL for (BBRC),
 222 26.22 ELISA units/mL for Q2 Solutions). Both laboratories used the same
 223 protocol and material for the assay.

224

225 In Figure 1 the dynamics of antibody concentrations (median and in-
 226 terquartile ranges) per vaccination group is given, considering data from the
 227 three studies pooled together (for further details, see supplementary Figure
 228 S1 and supplementary Table S1).

229

230 **3. Mathematical model for primary and anamnestic response**

231 *3.1. Model formulation*

232 To capture the establishment of the humoral immune response to a two-
 233 dose vaccination regimen and predict the reaction to a booster immunization
 234 we propose a mathematical model based on a system of five ODEs (Equations
 235 (1)-(5)). We consider three B cell populations: memory B cells (M), short-
 236 lived antibody secreting cells (S) and long-lived antibody secreting cells (L).
 237 In addition, we consider the concentration of antigen (A), which is introduced
 238 through immunizations, and causes primary as well as secondary responses.
 239 Finally, antibody concentration (Ab) is also described. For the sake of sim-
 240 plicity, we will denote this model as (MSL): a schematic representation is
 241 given in Figure 2. Equations of our model are:

$$(MSL) = \begin{cases} \dot{A} = -\delta_A A & (1) \\ \dot{M} = \tilde{\rho} A - (\tilde{\mu}_S + \tilde{\mu}_L) AM - \delta_M M & (2) \\ \dot{S} = \tilde{\mu}_S AM - \delta_S S & (3) \\ \dot{L} = \tilde{\mu}_L AM - \delta_L L & (4) \\ \dot{Ab} = \theta_S S + \theta_L L - \delta_{Ab} Ab & (5) \end{cases}$$

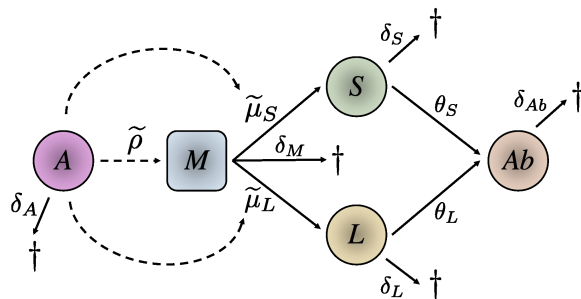


Figure 2: Schematic representation of (MSL) model. A stands for vaccine antigen, M for memory B cells, S for short-lived ASCs, L for long-lived ASCs, and Ab for specific soluble antibodies. See text and Equations (1)-(5) for details.

242 The reaction is initiated when a certain amount of antigen A is detected
 243 by the host immune defenses at time $t = 0$ (corresponding to the time of an
 244 immunization). The free antigen is progressively processed and eliminated

245 from the system with the per capita rate δ_A (Equation (1)). The antigen dy-
 246 namic is described by a simple exponential decay, because in this particular
 247 context neither of the two vaccine vectors are replicating [11]. The presence
 248 of antigen causes the instantaneous generation of M cells at rate $\tilde{\rho}A$, con-
 249 densing the complex biological process of activation of specific naïve B cells,
 250 and their subsequent massive proliferation and maturation within GCs. The
 251 M compartment is then an “hybrid” one. While the reaction is ongoing, M
 252 cells differentiate into both short- and long-lived ASCs, at rates $\tilde{\mu}_S$ and $\tilde{\mu}_L$
 253 respectively. After total antigen consumption, M denotes memory B cells
 254 (BMEMs), ready to differentiate into ASCs upon subsequent antigen stim-
 255 ulation. ASCs are ultimately differentiated cells which do not proliferate.
 256 They die with rate δ_S and δ_L , respectively. Antibodies are produced by both
 257 populations of ASCs in different proportions ($\theta_S S + \theta_L L$). Their half-life is
 258 described by parameter δ_{Ab} . Description of all parameters can be found in
 259 Table 2.

260

261 After some time, the reaction reaches a peak, then the production of new
 262 ASCs and BMEMs decreases and finally ends. Long-lived ASCs continue
 263 to produce antibodies assuring long-term immunity, while BMEMs persist in
 264 the organism to promote anamnestic responses in case of subsequent encoun-
 265 ters with the same antigen. Indeed, in this case, BMEMs can differentiate
 266 into antigen-specific ASCs and produce high-affinity antibodies.

267

268 3.2. Rescaled system

269 Compartment A is not observed in practice. In order to circumvent this
 270 difficulty, and to avoid identifiability issues (see Section 4), we can use the
 271 analytical solution of Equation (1) in Equations (2) to (5). We get:

$$\begin{cases} \dot{M} = \rho e^{-\delta_A t} - (\mu_S + \mu_L) e^{-\delta_A t} M - \delta_M M \\ \dot{S} = \mu_S e^{-\delta_A t} M - \delta_S S \\ \dot{L} = \mu_L e^{-\delta_A t} M - \delta_L L \\ \dot{Ab} = \theta_S S + \theta_L L - \delta_{Ab} Ab \end{cases} \quad (6)$$

272 Note that through this transformation the unknown parameters are $\rho :=$
 273 $\tilde{\rho}A_0$, $\mu_S := \tilde{\mu}_S A_0$, $\mu_L := \tilde{\mu}_L A_0$ instead of $\tilde{\rho}$, $\tilde{\mu}_S$ and $\tilde{\mu}_L$, where $A_0 := A(t=0)$.

Table 2: Description of model parameters with units. We represent by $[A]$ the unit of antigen concentration: this quantity has not been measured in any study considered here.

Parameter	Description	Unit
δ_A	Antigen declining rate	days ⁻¹
$\tilde{\rho}$	Rate at which M cells are generated over time per antigen concentration	IgG-ASC.(10 ⁶ PBMC) ⁻¹ .days ⁻¹ .[A] ⁻¹
$\tilde{\mu}_S$	Differentiation rate of M cells into S cells per antigen concentration	days ⁻¹ .[A] ⁻¹
$\tilde{\mu}_L$	Differentiation rate of M cells into L cells per antigen concentration	days ⁻¹ .[A] ⁻¹
δ_M	Declining rate of M cells	days ⁻¹
δ_S	Death rate of S cells	days ⁻¹
δ_L	Death rate of L cells	days ⁻¹
θ_S	Antibody production rate per S cells	ELISA Units.mL ⁻¹ .(IgG-ASC) ⁻¹ 10 ⁶ PBMC.days ⁻¹
θ_L	Antibody production rate per L cells	ELISA Units.mL ⁻¹ .(IgG-ASC) ⁻¹ 10 ⁶ PBMC.days ⁻¹
δ_{Ab}	Antibody death rate	days ⁻¹

274 *3.3. Special case: no memory cells death*

275 It has been reported in the literature that BMEMs are an exceptionally
 276 stable population [48, 49]. It is hence reasonable to assume that $\delta_M \ll 1$.
 277 Let us consider the rescaled system (6). Under the assumption $\delta_M = 0$, there
 278 exists a stationary state reached by BMEMs, given by:

$$M \stackrel{\delta_M=0}{=} \frac{\rho}{\mu_S + \mu_L} \quad (7)$$

279 The state (7) is globally asymptotically stable [50]. The assumption
 280 $\delta_M \ll 1$ will be useful to interpret results in Sections 5 and 7. However,
 281 there is no constraint on this parameter in the sequel.

282
 283 It is worth noting that in the case $\delta_M > 0$, the M population will converge
 284 exponentially towards 0. Nevertheless, provided that $\delta_M \ll 1$ and in

285 particular $\delta_M \ll \delta_{Ab}$, the decreasing slope of M will be very small, hence the
 286 effect of δ_M will barely affect the Ab dynamics during the observation period.

287 3.4. Special case: absence of antigen stimulation

288 The model developed here extends a model proposed in [42] and applied
 289 in [47] in the context of the EBOVAC1 project to analyze the antibody
 290 response after the second dose. In these works the authors hypothesized
 291 that their observations began when the B cell response was already in the
 292 declining phase, *i.e.* there was no further generation of ASCs. In the absence
 293 of antigenic stimulus (*e.g.* $A_0 = 0$), (6) reduces to:

$$\left\{ \begin{array}{l} \dot{M} = -\delta_M M \\ \dot{S} = -\delta_S S \\ \dot{L} = -\delta_L L \\ \dot{Ab} = \theta_S S + \theta_L L - \delta_{Ab} Ab \end{array} \right. \begin{array}{l} (8) \\ (9) \\ (10) \\ (11) \end{array}$$

294 This corresponds to the model used in [42, 47], with the addition of Equa-
 295 tion (8) which does not affect Equations (9)-(11).

297 3.5. Simulating the response to subsequent stimulations

298 The (MSL) model allows to describe the establishment of the humoral
 299 response by the first dose of antigen. To simulate the response to the second
 300 dose and subsequent stimulations, vaccine antigen is added to compartment
 301 A according to the vaccination schedule. Hence, the (MSL) model is applied
 302 again with predicted values of M , S , L and Ab the day of the planned sec-
 303 ond dose as new initial conditions. This can be mathematically formalized
 304 as follows.

305
 306 Let n be the number of vaccine doses; t_i , $i = 1, \dots, n$ the time of ad-
 307 ministration of the i^{th} -dose and t_{n+1} the last observation time. Let $\psi_i :=$
 308 $(\delta_{A,i}, \rho_i, \delta_{M,i}, \mu_{S,i}, \mu_{L,i}, \delta_{S,i}, \delta_{L,i}, \theta_{S,i}, \theta_{L,i}, \delta_{Ab,i})$ be the vector of unknown pa-
 309 rameters associated with the immune response to the i^{th} -dose. We denote
 310 the initial conditions by M_0, S_0, L_0, Ab_0 .

311
 312 For $t_i < t \leq t_{i+1}$, $i = 1, \dots, n$, the dynamics of M, S, L, Ab following the
 313 i^{th} -immunization is obtained as the solution to the following ODE system:

$$\begin{cases} \dot{M} = \rho_i e^{-\delta_{A,i}(t-t_i)} - (\mu_{S,i} + \mu_{L,i}) e^{-\delta_{A,i}(t-t_i)} M - \delta_{M,i} M \\ \dot{S} = \mu_{S,i} e^{-\delta_{A,i}(t-t_i)} M - \delta_{S,i} S \\ \dot{L} = \mu_{L,i} e^{-\delta_{A,i}(t-t_i)} M - \delta_{L,i} L \\ \dot{Ab} = \theta_{S,i} S + \theta_{L,i} L - \delta_{Ab,i} Ab \end{cases}, \quad (12)$$

314 with initial conditions: $M_0 = M(t = t_i), \dots, Ab_0 = Ab(t = t_i)$.

315 4. Identifiability analysis

316 We have performed a theoretical study of the rescaled model described
317 by (6) to determine which biological data are needed to accurately estimate
318 parameters and infer predictions about two-dose vaccination regimens.

319
320 *A priori* structural identifiability is a structural property of a model. It
321 ensures a sufficient condition for recovering uniquely unknown model param-
322 eters from knowledge of the input-output behavior of the system under ideal
323 conditions (*i.e.* noise-free observations and error-free model structure). We
324 refer to Miao *et al.* [51] for a formal definition of *a priori* structural identi-
325 fiability.

326
327 Ideally one would assess global structural identifiability, but sometimes
328 local identifiability can be sufficient if *a priori* knowledge on the unknown
329 parameters allows to reject alternative parameter sets. For instance, global
330 identifiability for (6) would not be reached without imposing any condition
331 on the half-life of compartment S compared to L . Indeed, from a structural
332 point of view, the roles of S and L are perfectly symmetric.

333
334 We assess local structural identifiability of (6) using the **IdentifiabilityAnalysis**
335 package implemented in Mathematica (Appendix A). We sup-
336 pose that $Ab_0 = Ab(t = 0)$ is known and $Ab(t)$ is observed during follow-up,
337 which is consistent with available data (Section 2). If all other initial con-
338 ditions are unknown, (6) results in being non-identifiable (Supplementary
339 Table S2). The non-identifiable parameters are $L_0, M_0, S_0, \mu_L, \mu_S, \rho, \theta_L,$
340 θ_S , with degree of freedom 2. This means that, in order to solve the non-
341 identifiability issue, one should fix at least two parameters within the set of
342 non-identifiable parameters, $\{\mu_L, \mu_S, \rho, \theta_L, \theta_S\}$. However, there is no avail-
343 able information on the values of these parameters, hence they cannot be

344 fixed *a priori*. Therefore, additional biological data corresponding to other
345 compartments need to be integrated to ensure structural identifiability.

346

347 Analyses of specific B cell response induced by vaccination could be per-
348 formed through the Enzyme-Linked Immunosorbent Spot Assay (ELISpot).
349 This is a sensitive method to identify the concentration of antigen-specific
350 ASCs [52]. Antigen-specific BMEMs can also be analyzed through the ELISpot
351 techniques, but this requires *ex vivo* polyclonal activation over 3 to 8 days
352 before detectable amounts of antibodies can be found.

353

354 Specific ASCs correspond in (6) to $(S + L)(t)$. Let us assume they
355 are measured during follow-up; baseline values of both S and L are still
356 supposed unknown. We obtain that Model (6) with unknown parameter
357 vector $\psi := (\delta_A, \rho, \mu_S, \mu_L, \delta_M, \delta_S, \delta_L, \theta_S, \theta_L, \delta_{Ab})$, and outputs vector $\mathbf{y}(t) =$
358 $(Ab_0, Ab(t), (S + L)(t))$ is *a priori* structurally identifiable (Supplementary
359 Table S2).

360

361 Let us assume that the M compartment is observed during follow-up
362 instead of $S + L$. In this case, the structural identifiability of Model (6) is
363 not ensured, according to the `IdentifiabilityAnalysis` algorithm (Supple-
364 mentary Table S2). Other parameters should be fixed or information about
365 ASCs should be integrated.

366

367 We can conclude that $\{Ab_0, Ab(t), (S + L)(t)\}$ is a suitable minimal out-
368 put set to be considered to ensure model identifiability. Of course any other
369 additional information about parameters and/or model compartments will
370 increase the identifiability of (6) and the reliability of parameter estimation.

371

372 Of note, this analysis of theoretical identifiability still does not guarantee
373 practical identifiability, which depends on availability and quality of data [51],
374 such as time point distribution of measurements and measurements errors.
375 However, practical identifiability could be improved by using a population
376 approach for parameter estimation based on mixed-effects models [53, 54, 55].
377 This approach allows to perform parameter estimation across a whole pop-
378 ulation of individuals simultaneously, and quantify the variations that some
379 covariates (either categorical and continuous) of interest produce over the
380 dynamics of specific subgroups (*e.g.* heterogeneous vaccination schedules).
381 This is done by assuming some underlying structure to the distribution of

382 individual-level parameters across a population. Firstly, each individual pa-
383 rameter is described by an intercept representing the mean parameter value
384 across the whole population. Then, part of variability can be described by
385 way of covariates allowing the distinction between different sub-populations,
386 and finally a normally distributed random effect characterizes the remain-
387 ing between-subjects unexplained variability. Within this framework, either
388 maximum likelihood and Bayesian approaches has been proposed to perform
389 parameter estimation.

390

391 5. Model calibration

392 Model (6) is not structurally identifiable with the observation of com-
393 partment Ab only: a reliable parameter estimation cannot be performed.
394 Therefore, we propose a model calibration against antibody concentration
395 data to assess the ability of (6) to reproduce antibody kinetics consistent
396 with available experimental data.

397 5.1. Methods

398 To perform the calibration, we considered the antibody concentration
399 data as described in Section 2.

400

401 We calibrated (6) considering the median and interquartile ranges among
402 all studies pooled together stratified by vaccination group, considering vac-
403 cination group Ad26/MVA D57 as the reference group.

404

405 $M(0)$, $S(0)$, $L(0)$ and $Ab(0)$ were set equal to 0 before the first dose,
406 *i.e.* we supposed there were no previously existing specific antibodies nor
407 B cells. Initial conditions of the reaction to the second dose are set as the
408 predicted values of each compartment at the second dose immunization day,
409 as described in Section 3.5. Simulations of (6) have been performed using
410 Matlab, `ode45` function. According to biological assumptions or previous
411 modeling results, we suppose that the following parameters could be modified
412 depending on the vaccine vector and/or the timing of dose administration
413 (see Table 3 for notation details):

- 414 • ρ, μ_S, μ_L are vector dependent (Ad26.ZEBOV or MVA-BN-Filo). These
415 parameters determine the strength of the humoral response and the

416 amount of ASCs and BMEMs generated (Section 3). Biological evi-
 417 dences suggest that the strength and quality of the immune response
 418 is dependent on the type of antigen inducing the reaction and the way
 419 it is presented (*e.g.* [56]).

420 • $\delta_S(\text{PVD1}) \geq \delta_S(\text{PVD29}) \geq \delta_S(\text{PVD57})$: Pasin *et al.* [47] have identi-
 421 fied a significant effect of the delay between immunizations on δ_S by
 422 analyzing the same phase I data we are considering here, with a sim-
 423 plified mechanistic model.

424 • $\delta_S(\text{Ad26}) \neq \delta_S(\text{MVA})$: the effect of the order of administration of vac-
 425 cine vector over the decay rate of short-lived ASCs has been evidenced
 426 in a previous analysis by Pasin *et al.* [47]. The higher complexity of
 427 the model described here allows to define a direct dependence between
 428 parameters and vaccine vectors: we allow parameter δ_S to change ac-
 429 cording to the vaccine vector used.

430 • $\rho(\text{PVD1}) < \rho(\text{PVD29}) \leq \rho(\text{PVD57})$: the secondary response is im-
 431 proved in magnitude with respect to the primary one, due to the pres-
 432 ence of specific BMEMs contributing to the initiation of GCs reaction
 433 in a more effective way [29]. Parameter ρ determines the strength of
 434 the humoral response because it defines the generation of M cells upon
 435 antigen stimulation, *i.e.* the GC reaction breadth. Therefore M cells
 436 do not play exactly the same role when a primary (GCs generated
 437 from activated naïve B cells) or a secondary (GCs seeded by BMEMs
 438 or newly activated naïve B cells; BMEMs differentiating into ASCs) re-
 439 sponse is simulated [22, 28], hence it is reasonable to allow parameter ρ
 440 to increase from the first immunization ($\rho(\text{PVD1})$) to the following one
 441 ($\rho(\text{PVD29})$ or $\rho(\text{PVD57})$). In addition, previous studies on different
 442 viruses and vaccines have shown that an increased interval between im-
 443 munizations is associated with an improved magnitude of the response
 444 (*e.g.* [57, 58]). Consequently, an additional variation of parameter ρ
 445 depending on the interval between the two doses is permitted.

446 • $\delta_A(\text{Ad26}) \leq \delta_A(\text{MVA})$: according to biodistribution and persistence re-
 447 sults, Ad26 is cleared in approximately 3 months [59], while MVA is
 448 cleared in approximately 1 month [60]. Note that here antigen concen-
 449 tration defines the duration of the GC response, so it does not exactly
 450 reflect biodistribution.

Table 3: Let ψ be a generic (unknown) parameter in $\{\delta_A, \rho, \mu_S, \mu_L, \delta_M, \delta_S, \delta_L, \theta_S, \theta_L, \delta_{Ab}\}$. If it is dependent on the interval between immunizations or vaccine vector we write $\psi(\text{cat})$, “cat” being a possible category of each variability factor.

		$\psi(\text{cat})$
Factor	Category	Meaning
Timing	PVD1	Post vaccination at day 1
	PVD29	Post second vaccination at day 29
	PVD57	Post second vaccination at day 57
Vaccine vector	MVA	The vaccine vector is MVA-BN-Filo
	Ad26	The vaccine vector is Ad26.ZEBOV

451 Model calibration has been achieved by repeated simulations of (6) and
 452 parameter tuning, until we obtained a consistent parameter set able to repro-
 453 duce reasonable antibody dynamics in accordance with interquartile ranges
 454 of experimental data for all vaccination groups.

455 5.2. Results

456 Table 4 shows parameter values obtained at the end of the calibration
 457 process described in Section 5.1.

458
 459 In Figure 3, antibodies (Figure 3 (a)) and ASCs and BMEMs (Figure 3
 460 (b)) dynamics are plotted for the reference vaccination group, Ad26/MVA
 461 D57, as an example. Results for all other vaccination groups are given in
 462 supplementary Figures S2-S3. The time axis is rescaled at the day of the
 463 primary injection (*i.e.* study day 1) and simulations performed up to 1 year
 464 after the first dose.

465
 466 In Figure 3 (a), orange dots correspond to median values of antibody
 467 concentrations data from the corresponding vaccination group. We were able
 468 to satisfactorily reproduce antibody concentrations dynamics in accordance
 469 with experimental observations for all vaccination groups. In supplementary
 470 Table S3 further details are given, with comparison of simulations to real
 471 data at some point of interest, *e.g.* at the time of the observed antibody
 472 peak and one year after the first dose.

473

Table 4: Parameters set obtained through (MSL) model calibration and used for simulations plotted in Figure 3 and supplementary Figures S2-S3. The half-life corresponding to rate loss parameters is given by: $t_{1/2}(\delta_i) := \ln(2)/\delta_i$. Structurally identifiability of parameters with antibody concentrations observations is recalled, according to results of Section 4 (Y=structurally identifiable; N=structurally non-identifiable)

Parameter	Prior	Ref.	Value		Unit	Structurally identifiable with measured <i>Ab</i> only?
			Ad26	MVA		
$t_{1/2}(\delta_A)$	-	-	10.7	3.3	days (half-life is derived from the approximate time to clear Ad26.ZEBOV and MVA-BN-Filo respectively : $t_{1/2}(\delta_A)(\text{Ad26}) > t_{1/2}(\delta_A)(\text{MVA})$ [59, 60])	Y
ρ	-	PVD1 PVD29 PVD57	3.5	0.7	IgG-ASC/ 10^6 PBMC.days $^{-1}$	N
			15	17		
			15	20		
μ_S	-		2.5	0.4	days $^{-1}$	N
μ_L	-		0.011	0.0035	days $^{-1}$	N
$t_{1/2}(\delta_M)$	≥ 50	[49]	63.3		years	Y
$t_{1/2}(\delta_S)$	-	PVD1 PVD29 PVD57	0.7	0.7	days	Y
			2.8	4.6		
			4.6	11.6		
$t_{1/2}(\delta_L)$	[2.7;13]	[47]	9.5		years	Y
θ_S	-		20		ELISA Units/mL.(IgG-ASC/ 10^6 PBMC) $^{-1}$.days $^{-1}$	N
θ_L	-		30		ELISA Units/mL.(IgG-ASC/ 10^6 PBMC) $^{-1}$.days $^{-1}$	N
$t_{1/2}(\delta_{Ab})$	[22;26]	[47]	23.9		days	Y

474 The model predicts that antibody levels at one year after the first dose
475 are comparable among all vaccine regimens, in accordance with data. The
476 antibody response peak has been measured 21 days after the second dose.
477 Antibody dynamics obtained with our calibration show a slightly delayed
478 peak between 3 and 4 weeks after the second dose. Of note, no immuno-
479 genicity measurements have been performed *e.g.* at 2 weeks nor at 4 weeks.

480
481 In Figure 3 (b) the dynamics of B cells are plotted: for ASCs, we consider
482 the sum of short- and long-lived ASCs. Note that, because the half-life of
483 short-lived B cells is supposed to be significantly shorter than long-lived B
484 cells one, at 1 year of follow-up we do not have any contribution from the S
485 compartment.

486
487 Results about B cell subsets dynamics correspond only to model predic-
488 tions since they were not calibrated on real data, therefore model parameters
489 could not be accurately determined. However, with the data available so far
490 from phase I studies, this model provides a good starting point and it will
491 be further implemented and validated when additional biological data on B-
492 cells populations from ongoing phase II and phase III clinical studies will be
493 available. ASCs dynamic shows an early peak located a few days (between 7
494 to 10) after the second dose. This is in accordance with other studies assess-
495 ing B cell kinetics upon vaccination (*e.g.* [26, 27]). It is followed by a rapid
496 relaxation phase, then stabilization.

497
498 The rapid decreasing slope after the peak of the ASCs response (*i.e.*
499 from approximatively 1 to 10 weeks after the second dose) depends on the
500 value of parameter δ_S , which corresponds to a very small half-life of short-
501 lived ASCs (varying from almost 3 to 12 days, depending on the regimen).
502 The concentration of long-lived ASCs is low for the obtained parameter set,
503 but able to sustain the antibody response due to the long half-life of this
504 population. BMEM level depends on parameters ρ, μ_S and μ_L , as stressed
505 in Section 3.3 (note that according to Table 4 the half-life of M cells is set
506 here at about 63 years, which implies a really weak value for parameter δ_M ,
507 of the order of 10^{-5}).

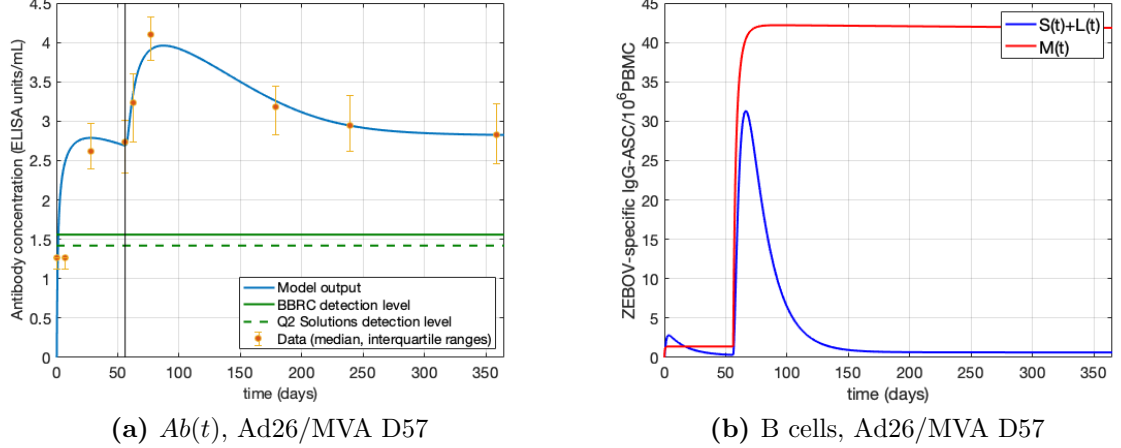


Figure 3: Predictions from the calibrated (MSL) model for the reference group, Ad26/MVA D57. **(a)** Antibody concentrations (\log_{10} -transformed). Green horizontal lines denote detection levels used by the BBRC laboratory (solid line) and by the Q2 Solutions laboratory (dashed line) respectively. **(b)** B cells. S and L stand for short-lived and long-lived ASCs respectively; M represents BMEMs.

508 6. Sensitivity analysis of the antibody compartment

509 We have obtained a parameter set able to reproduce antibody responses
 510 dynamics to two-dose vaccine regimens against Ebola virus that closely re-
 511 semble experimental observations. We perform a local sensitivity analysis
 512 of the antibody compartment to clarify the effect of each parameter on it
 513 over time. This can help detecting two different sources of practical non-
 514 identifiability of parameters:

- 515 1. a very weak effect of a given parameter on the observed compartment
 516 or an effect which is concentrated in a specific time window where
 517 observations are very scarce;
- 518 2. the interplay among parameters: the effect of the variation of one pa-
 519 rameter on the observed compartment can be compensated by a suit-
 520 able variation of another parameter.

521 An intuitive representation of local sensitivity of the Ab compartment
 522 with respect to each parameter is given by the evaluation of curves $\phi_{\psi_i}(t) :=$

$$523 \frac{\psi_i}{Ab(t, \psi)} \frac{\partial Ab(t, \psi)}{\partial \psi_i} \Big|_{\psi = \psi^*}, \text{ for each parameter } \psi_i \text{ in } \psi = \{\delta_A, \rho, \delta_M, \mu_S, \mu_L, \delta_S, \delta_L, \theta_S, \theta_L, \delta_{Ab}\}$$

524 [61]. The quotient ψ_i/Ab is introduced to normalize the coefficient and avoid
 525 influence of units.

526

527 6.1. Results

528 Partial derivatives of (6) Ab output with respect to each parameter are
 529 numerically evaluated (Appendix B). ψ^* is set at parameter values corre-
 530 sponding to the reference regimen, Ad26/MVA D57 (Table 4). In Figure 4,
 531 $\phi_{\psi_i}(t)$ for all ψ_i in ψ are plotted. The time axis is rescaled at the day of the
 532 second dose administration.

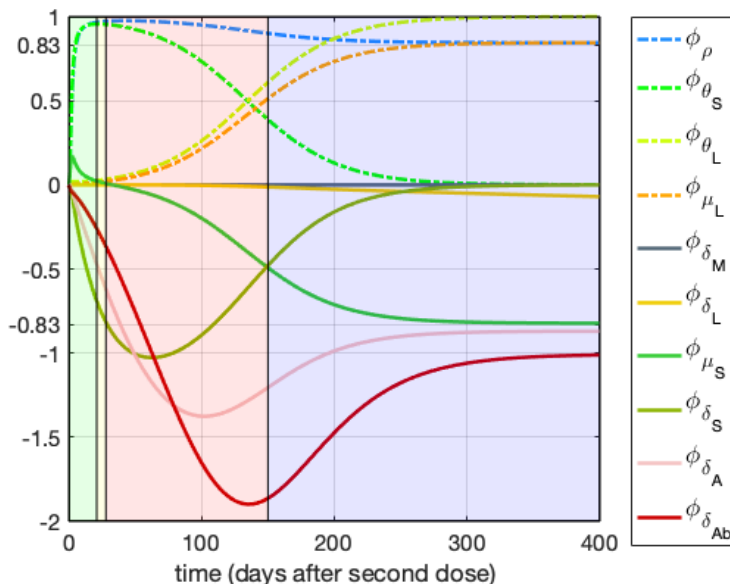


Figure 4: Relative sensitivity of the Ab compartment with respect to (MSL) parameters over time. For each parameter ψ_i in $\psi = \{\rho, \theta_S, \delta_S, \delta_A, \delta_{Ab}, \theta_L, \mu_S, \mu_L, \delta_M, \delta_L\}$ the normalized sensitivity coefficients are plotted: $\phi_{\psi_i}(t) := \frac{\psi_i}{Ab(t, \psi)} \frac{\partial Ab(t, \psi)}{\partial \psi_i} \Big|_{\psi = \psi^*}$. For the sake of clarity we shade differently time windows corresponding to distinct phases of the antibody kinetics: in green the first exponential phase, in yellow the antibody peak, in pink the declining phase, in blue the stabilization phase.

533

534 The influence of almost all parameters over Ab dynamics significantly
 535 changes over time. In particular, in the very early exponential phase after

536 vaccine immunization, parameters that mostly influence the antibody re-
 537 sponse in (6) are ρ , which determines the intensity of the immune response
 538 upon antigen stimulation, and θ_S and δ_S , characterizing the antibody pro-
 539 duction rate of short-lived ASCs and their half-life respectively. Right after
 540 the antibody peak, the most relevant parameters are the decay rate of antigen
 541 δ_A and the half-life of antibodies δ_{Ab} . Asymptotically, we will mostly retain
 542 the influence of δ_{Ab} and the antibody production rate of long-lived ASCs θ_L
 543 (even if δ_A , ρ , and the differentiation rates of M cells into both compartments
 544 of ASCs, μ_S and μ_L , also have a great influence).

545
 546 From curves plotted in Figure 4 it is also possible to deduce in which
 547 direction each parameter affects the Ab dynamics: increasing the values of
 548 ρ , μ_L , θ_S and θ_L implies an increase in Ab concentration. The loss rates
 549 δ_A , δ_S , δ_{Ab} , δ_L and parameter μ_S (starting from a few weeks post vaccination)
 550 acts in the opposite way: an increase of their values is associated to a de-
 551 crease of the Ab concentration. Note that the sensitivity of Ab with respect
 552 to μ_S is positive during the first weeks after vaccination, because this param-
 553 eter determines the generation of short-lived ASCs, which govern the early
 554 antibody response.

555
 556 The half-lives of both M and L populations are supposed to be signifi-
 557 cantly greater than antibody half-life. This explains why parameters δ_M and
 558 δ_L have an extremely low influence over Ab dynamics on the one-year period
 559 considered and locally around parameter set given in Table 4. The reliability
 560 of their estimations could be refined either by considering longer follow-up
 561 or by integrating data related to these compartments (*cf.* specific BMEMs
 562 and ASCs through the ELISpot technique).

563
 564 Finally, Figure 4 shows that in absolute value, the sensitivity of Ab with
 565 respect to some parameters seems to asymptotically stabilize at the same
 566 value (starting from approximately 250 days after the second dose). We are
 567 referring to *e.g.* (ρ, μ_L) in the same way, and (δ_{Ab}, θ_L) in opposite ways. This
 568 has consequences on the identifiability of these parameters: the effect of the
 569 variation of one among them can be compensated by a suitable variation of
 570 its pair, at least over some specific time windows. This implies that if an-
 571 tibody observations are collected exclusively within these time windows, it
 572 would not be possible to accurately estimate these parameters individually,
 573 due to their interplay.

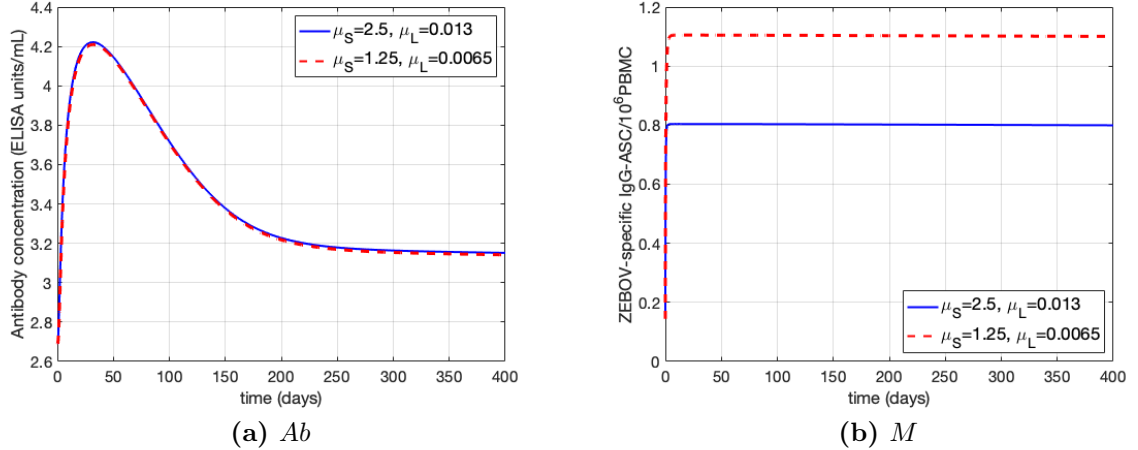


Figure 5: Effects of a variation of both μ_S and μ_L of 50% on **(a)** Ab and **(b)** M (all other parameters are fixed as in Table 4).

574

575 A particular focus should be made on parameters μ_S and μ_L : the sensi-
 576 tivity of Ab with respect to these parameters is symmetric (in opposite way)
 577 over time starting early (few weeks) after immunization. Henceforth the Ab
 578 dynamics will be unchanged by preserving the quotient between μ_S and μ_L
 579 (note that (6) is not identifiable if the only observed compartment is Ab).
 580 In Figure 5 (a) we plot the Ab dynamics obtained when both μ_S and μ_L
 581 are increased by 50% simultaneously: we can see that the obtained curves
 582 are superposed. Nevertheless, the corresponding M dynamics is significantly
 583 affected by changes in the individual values of μ_S and μ_L , as shown in Figure
 584 5 (b). This further stress the importance of integrating further biological
 585 data to proceed to parameter estimation in a reliable manner.

586

587 6.2. Conclusions

588 Sensitivity analysis is used to gain a better understanding of the practical
 589 identifiability of model parameters from antibody concentrations data.

590

591 The sensitivity of antibody dynamics with respect to parameters δ_M and
 592 δ_L is extremely weak: changing their values does not affect significantly the
 593 Ab output, at least in the considered time window. We conclude that these

594 parameters are practically non-identifiable considering only antibody data
595 and one year of follow-up.

596

597 Parameters μ_S and μ_L are closely related, affecting antibody dynamics in
598 a symmetric way. Antibody concentration data would not allow their esti-
599 mation individually, due to their collinearity.

600

601 Other parameters will be practically non-identifiable due to data quality
602 (*e.g.* time point distribution and/or measurements errors and limitations).
603 In particular, one should pay particular attention to parameters which ex-
604 clusively describe the reaction to the first vaccine dose. Indeed, very few
605 antibody measurements are above the detection level before the second dose,
606 in particular for patients primed with MVA-BN-Filo (Section 2).

607 7. Simulations of a booster dose

608 One of the main interests in modeling the establishment and reactivation
609 of the immune response after multiple antigen exposures is the prediction of
610 the effects of a booster dose. With (6) we can expect to be able to predict
611 the strength of an anamnestic response by the mean of the establishment of
612 an effective immunological memory.

613

614 We use the calibrated model (6) to simulate the response to an Ad26.ZEBOV
615 booster dose, realized at day 360 after the first dose for vaccination group
616 Ad26/MVA D57.

617

618 In order to simulate the first two immunizations (*i.e.* the regular two-
619 dose schedule), we use the parameter set obtained in Section 5 (Table 4).
620 The Ad26.ZEBOV booster dose is simulated using the parameter set corre-
621 sponding to an Ad26.ZEBOV immunization 56 days after the first dose.

622

623 In Figure 6 we plot the dynamics of both antibodies (\log_{10} -transformed)
624 and B cells (ASCs and BMEMs) as predicted by (6) for the second dose and
625 booster immunizations. The time axis is rescaled to have time 0 correspond-
626 ing to the second immunization day (*i.e.* day 57). Further information is
627 given in supplementary Table S4.

628

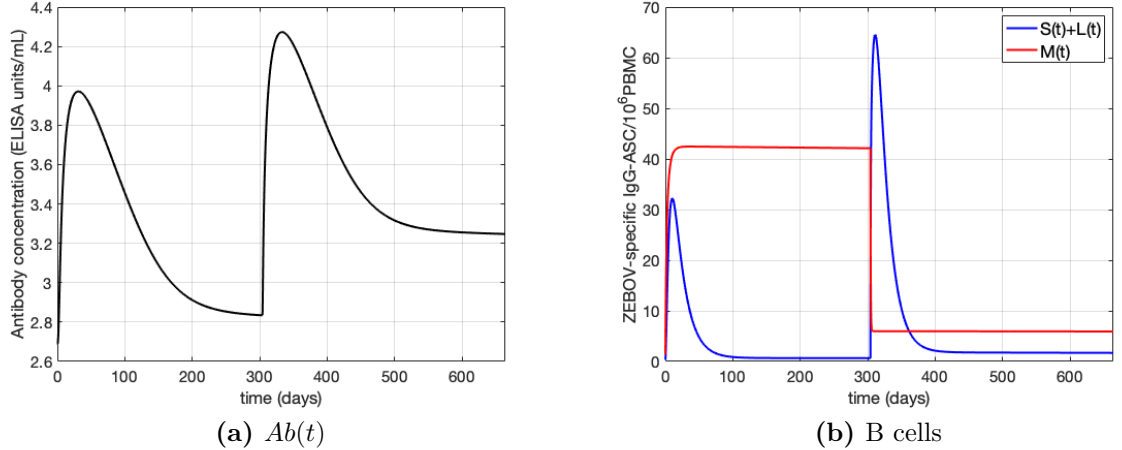
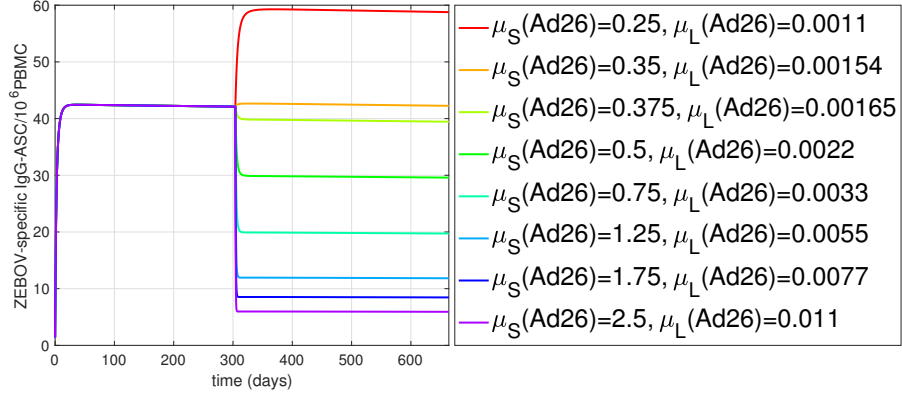


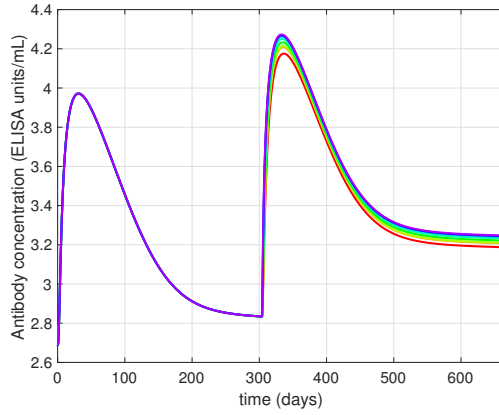
Figure 6: Simulation of (MSL) for vaccination group Ad26/MVA D57 with a booster dose of Ad26.ZEBOV one year after the first dose (day 360). In (a) the obtained \log_{10} -transformed antibody concentration is given. In (b) S and L stand for short-lived and long-lived ASCs respectively; M represents memory cells. The time axis is rescaled at the second dose day (*i.e.* day 57).

629 Simulations show a strong humoral anamnestic response to the booster
 630 immunization, with approximately a 11-fold increase of antibody concentra-
 631 tion within 7 days post booster dose, and a 25-fold increase within 21 days
 632 (in linear scale). This is due to the presence of a high affinity pool of BMEMs
 633 which differentiate into ASCs directly upon antigen stimulation. In addition,
 634 the model predicts a 2.5-fold increase in antibody concentration 360 days af-
 635 ter the booster dose (*i.e.* day 720) compared to day 360.

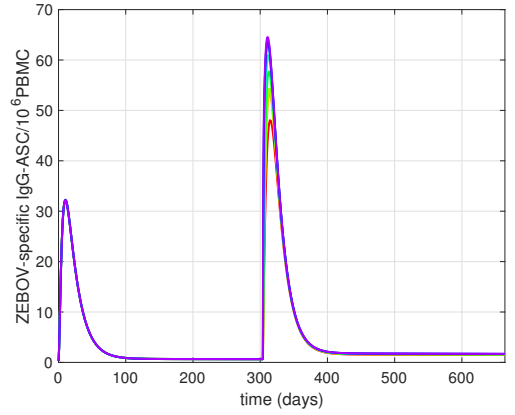
636
 637 In Figure 6 (b) we have plotted the corresponding B cell dynamics.
 638 Again, we observe that ASCs increase drastically after the booster immuniza-
 639 tion, hence stabilizes at a higher level than before, correlating with antibody
 640 concentrations. After the booster dose, BMEMs stabilize at a lower level:
 641 this depends on the calibrated values for parameters ρ , μ_S and μ_L under the
 642 assumption that the effect of Ad26.ZEBOV as booster dose would be similar
 643 to Ad26.ZEBOV at Day 57 as second dose. We anticipate that, from an im-
 644 munological perspective, depletion of BMEM (Figure 6 (b)) is not reflecting
 645 the immunological situation post booster dose, because replenishment of the
 646 BMEM compartment is to be expected after booster vaccination. Otherwise,



(a) $M(t)$



(b) $Ab(t)$



(c) $(S + L)(t)$

Figure 7: Simulation of (MSL) for vaccination group Ad26/MVA D57 with a booster dose of Ad26.ZEBOV one year after the first dose (day 360), when both $\mu_S(\text{Ad26})$ and $\mu_L(\text{Ad26})$ for the booster dose of Ad26.ZEBOV are varied by (from top to bottom, see legend in (a)) 90%, 86%, 85%, 80%, 70%, 50%, 30% from the reference value as in Table 4 (purple curve). In (a) the corresponding M dynamics are given, in (b) the \log_{10} -transformed antibody concentration and in (c) the ASCs dynamics. The time axis is rescaled at the second dose day (*i.e.* day 57).

647 this would mean that after a few encounters with the same antigen, instead of
 648 building up stronger immunity and memory like what is observed in real life
 649 for many pathogens [62, 63, 64], the memory would have a lower level. With
 650 these regards, we ran additional sensitivity analyses in which we decreased
 651 the values of the parameters μ_S and μ_L for the booster dose of Ad26.ZEBOV

652 down to 10-fold lower values (Figure 7). We show that, by modifying these
653 values the BMEMs (Figure 7 (a)) reach higher levels, while both the an-
654 tibody levels (Figure 7 (b)) and the plasma cells levels (Figure 7 (c)) are
655 similar for the different sets of parameters (μ_S, μ_L). Immunologically, the
656 variation of parameters μ_S and μ_L for the booster dose can be justified by
657 assuming a complete maturation (hence effectiveness upon antigen stimula-
658 tion) of the BMEMs only at the time of the booster (and not at dose 1/dose
659 2) [57, 58].

660
661 If experimentally confirmed, these results would suggest the establishment
662 of an effective immunological memory against Ebola virus, as a response
663 to the two-dose vaccine regimen. Model predictions about the effects of a
664 booster dose could be further evaluated when supplementary immunological
665 data from a subgroup of ongoing phase II clinical studies which received
666 booster dose of Ad26.ZEBOV will be available [65].

667 8. Discussion

668 Recurring Ebola outbreaks have been recorded in equatorial Africa since
669 the discovery of Ebola virus in 1976, with the largest and more complex
670 one occurred in West Africa between March 2014 and June 2016. We are
671 now currently experiencing, in the DRC, the second largest outbreak ever
672 recorded. A prophylactic vaccine against Ebola virus is urgently needed.

673
674 A new two-dose heterologous vaccine regimen against Ebola Virus based
675 on Ad26.ZEBOV and MVA-BN-Filo developed by Janssen Vaccines & Pre-
676 vention B.V. in collaboration with Bavarian Nordic is being evaluated in
677 multiple clinical studies. The immune response following vaccination has
678 been mainly assessed through specific binding antibody concentrations (Sec-
679 tion 2). The level of circulating antibodies needed to ensure protection is
680 currently unclear: persistence of antibody responses after the two-dose vac-
681 cination has been clinically observed up to one year after the first dose, yet
682 at a lower level than shortly after vaccination. Since we don't currently know
683 for how long the two-dose vaccine can convey protection, a booster vaccina-
684 tion can be considered in case of imminent risk of exposure to Ebola virus
685 (pre-exposure booster vaccination).

686

687 We proposed an original mechanistic ODE-based model - (MSL) - which
688 takes into account the immunological memory (BMEMs) and short- and long-
689 lived ASCs dynamics (Section 3). This model, which is an extension of the
690 model developed by Andraud *et al.* [42], aimed at explaining the primary
691 response after receiving a first vaccine dose against Ebola virus, and the se-
692 condary response following a second heterologous vaccine dose. The final
693 goal of our model is to predict the speed and magnitude of the anamnes-
694 tic response triggered by a booster vaccination among individuals who have
695 been vaccinated with the two-dose regimen, and the long-term antibody per-
696 sistence afterward. Succeeding in this task will be extremely helpful to better
697 understand the immune response to a vaccine regimen.

698
699 We have performed structural identifiability analysis of (MSL) model
700 (Section 4), which pointed out that antibody concentrations data are not
701 sufficient to ensure (MSL) structural identifiability. Indeed, different param-
702 eter sets can reproduce the same antibody dynamic. In order to proceed
703 with proper parameter estimation, at least ASCs data should be integrated.
704 Alternatively, some parameters should be fixed to allow estimation of the
705 remaining ones.

706
707 In the absence of priors on structural non-identifiable parameters and of
708 additional biological data, we decided to proceed to model calibration (Sec-
709 tion 5). To perform (MSL) model calibration, we have repeatedly simulated
710 (MSL) using Matlab and compared the *Ab* output to median and interquar-
711 tile ranges of available ELISA data from all studies pooled together, stratified
712 by vaccination group. We have shown that (MSL) model is able to reproduce
713 qualitatively the observed antibody kinetics for a well-chosen set of param-
714 eters. This provides the rationale to test the ability of (MSL) in predicting
715 the speed and magnitude of the immune response to a booster vaccine dose.

716
717 Based on parameter values obtained through (MSL) model calibration,
718 we have performed local sensitivity analysis to assess to which extent each
719 parameter affects antibody dynamics over time (Section 6). Hence, a better
720 insight on practical identifiability of model parameters has been achieved in
721 a sensitivity-based manner.

722
723 Finally, the calibrated model has been used to evaluate *in silico* a booster
724 dose of Ad26.ZEBOV one year after the first dose (Section 7), showing a

725 strong humoral anamnestic response. If experimentally confirmed, this would
726 increase confidence on the capacity of the proposed prophylactic regimen to
727 induce a robust and durable immune response against Ebola virus.

728

729 In order to simplify the model structure, in (MSL) the M compartment
730 describes the GC reaction and the contribution of the BMEM population
731 to the immune response. Therefore, due to the intrinsic difference between
732 the primary and the secondary responses, M cells do not play exactly the
733 same role when a primary (GCs generated from activated naïve B cells) or a
734 secondary (GCs seeded by BMEMs or newly activated naïve B cells; BMEMs
735 differentiating into ASCs) response is simulated [22, 28]. For this reason, it is
736 reasonable to adjust some parameters (*e.g.* $\rho, \delta_S, \mu_S, \mu_L$) from one immuniza-
737 tion to the following one, eventually also based on the time between the two
738 doses. In particular, an improved antibody response has been experimentally
739 observed when the delay between the first and second doses is higher (*e.g.*
740 56 days schedule compared to 28 days). Therefore, according to sensitivity
741 analysis performed in Section 6, we suggest to investigate through modeling
742 the possibility of an increase of parameters ρ and μ_L when increasing the
743 time lapse between the two doses, the opposite for parameters μ_S and δ_S .
744 Note that the effect of timing of the second dose on the half-life of short-lived
745 ASCs has been already observed by Pasin and coauthors [47].

746

747 Moreover, due to (MSL) definition, if we do not change any parameter
748 among $\{\rho, \mu_L, \mu_S\}$ from the first to following doses, BMEMs level remains
749 almost unchanged (Section 3.3), while we expect an increase in the concen-
750 tration of BMEMs after the booster dose.

751

752 After vaccination, the existence of a plateau reached by functional persist-
753 ing BMEMs has been reported in the literature [49]. In (MSL) this plateau
754 is quickly reached, due to the fact that we do not consider here any inter-
755 mediate maturation step from naïve to activated to functional differentiated
756 cells: when the antigen is introduced in the system, the M compartment is
757 almost instantaneously filled. The main consequence is that the contribution
758 of this compartment to enhance the secondary response will be substantially
759 unchanged regardless the time delay between two subsequent vaccine immu-
760 nizations, in the situation in which no parameter modification is permitted.

761

762 Despite the simplifications in model structure, several identifiability is-

763 sues have been raised in Sections 4 and 6. Consequently, another limitation
764 of this study is that model parameters could not be accurately and univocally
765 determined.

766

767 The (MSL) model provides a good starting point to evaluate the humoral
768 immune response elicited by the proposed vaccination regimens. Several fu-
769 ture research directions can be suggested by this work. For instance, (MSL)
770 model can be further refined using future data that will be available from
771 ongoing phase II and III clinical studies, in particular regarding B cell pop-
772 ulations and immune response after a booster vaccination. Other questions
773 should be addressed *in silico*. In particular, (MSL) model could be gener-
774 alized by relaxing the assumption of replication deficient vaccine vectors to
775 allow the study of the immune response elicited by live attenuated vaccine
776 virus. Indeed, it would be interesting to test (MSL) with other vaccination
777 studies, to determine whether some parameters are independent from the type
778 of vaccine vector used.

779 9. Conclusion

780 In this work we set a mechanistic model - (MSL)- of the humoral immune
781 response to one or more vaccine immunizations, based on an ODE system
782 of 5 equations. It describes the interaction between the antigen delivered by
783 replication deficient vaccine vectors, BMEMs, ASCs (distinguishing two pop-
784 ulations differing by their respective half-lives) and produced antigen-specific
785 antibodies. We have analyzed model structure identifying which kind of bi-
786 ological data should be collected or alternatively which parameters should
787 be fixed to perform proper parameter estimations. By confronting (MSL)
788 with ELISA data from two-dose heterologous vaccination regimens against
789 Ebola virus, we show that the model is able to reproduce realistic antibody
790 concentration dynamics after the two-dose heterologous vaccination. This
791 provides the rationale to test the ability of (MSL) in predicting the speed
792 and magnitude of the immune response to a booster vaccine dose, as we show
793 in this paper, and investigate long-term antibody persistence. Our findings
794 raise interesting further questions. Some of them require further biological
795 data, in particular regarding B cell populations assessment. Also, one could
796 be interested in understanding if some model parameters are intrinsic prop-
797 erties of the immune response, hence could help describing the response to
798 natural infection. Other questions should be addressed *in silico* to explore

799 the interaction of additional immune components and their contribution to
800 the establishment, maintenance and reactivation of the immune response to
801 a repeatedly presented antigen.

802 **10. Acknowledgments**

803 We thank the members of the EBOVAC1 consortium, in particular the
804 principal investigators of the EBOVAC1 trials, Matthew Snape, Omu Anzala,
805 George Praygod, Zacchaeus Anywaine. We also thank Andrew Pollard and
806 Elizabeth Clutterbuck for scientific discussions.

807 In addition, we thank the members of the EBOVAC3 consortium and
808 in particular Rosalind Eggo, Niel Hens, Carl Pearson and Bart Spiessens,
809 involved in the modeling effort supporting the development of the two-dose
810 heterologous regimen developed by Janssen Vaccines & Prevention B.V., and
811 discussed in this paper.

812 This work has received funding from the Innovative Medicines Initiative
813 2 Joint Undertaking under Grant Agreement EBOVAC1 (No. 115854). This
814 Joint Undertaking receives support from the European Union’s Horizon 2020
815 research and innovation programme and EFPIA. The funder of the study had
816 no role in the study design, data collection, data analysis, data interpreta-
817 tion, or writing the report. The corresponding author had full access to all
818 the data in the study and had final responsibility for the decision to sub-
819 mit for publication. This work was also supported by the Investissements
820 d’Avenir program managed by the ANR under reference ANR-10-LABX-77.
821 The funder had no role in the study design, data collection, data analysis,
822 data interpretation, or writing the report.

823 Competing interests: TVE, VB and LS are employees of Janssen Phar-
824 maceuticals and may be Johnson & Johnson stockholders.

825 **References**

- 826 [1] W. E. R. Team, After ebola in west africa - unpredictable risks, pre-
827 ventable epidemics, *New England Journal of Medicine* 375 (6) (2016)
828 587–596.
- 829 [2] World Health Organisation, Ebola virus disease, Fact Sheet,
830 [https://www.who.int/news-room/fact-sheets/detail/ebola-](https://www.who.int/news-room/fact-sheets/detail/ebola-virus-disease)
831 [virus-disease](https://www.who.int/news-room/fact-sheets/detail/ebola-virus-disease), Last accessed on 2019-05-04 (2018).

- 832 [3] W. H. Organization, et al., Situation report: Ebola virus disease, 10
833 june 2016, World Health Organization, Geneva.
- 834 [4] W. H. Organization, et al., Ebola situation reports: Democratic republic
835 of the congo (2018).
- 836 [5] World Health Organisation, Ebola virus disease, Democratic Republic of
837 the Congo, External Situation Report N°82/2019, [https://www.who.
838 int/publications-detail/ebola-virus-disease-democratic-
839 republic-of-congo-external-situation-report-82-2019](https://www.who.int/publications-detail/ebola-virus-disease-democratic-republic-of-congo-external-situation-report-82-2019), Last
840 accessed on 2020-03-05 (2019).
- 841 [6] World Health Organisation, Statement on the meeting of the In-
842 ternational Health Regulations (2005) Emergency Committee for
843 Ebola virusdisease in the Democratic Republic of the Congo on
844 17 July 2019, [https://www.who.int/ihr/procedures/statement-
845 emergency-committee-ebola-drc-july-2019.pdf](https://www.who.int/ihr/procedures/statement-emergency-committee-ebola-drc-july-2019.pdf), Last accessed on
846 2019-07-23 (2019).
- 847 [7] T. Goldstein, S. J. Anthony, A. Gbakima, B. H. Bird, J. Bangura,
848 A. Tremeau-Bravard, M. N. Belaganahalli, H. L. Wells, J. K. Dhanota,
849 E. Liang, et al., The discovery of bombali virus adds further support for
850 bats as hosts of ebolaviruses, *Nature microbiology* 3 (10) (2018) 1084.
- 851 [8] L. Gross, E. Lhomme, C. Pasin, L. Richert, R. Thiebaut, Ebola vac-
852 cine development: Systematic review of pre-clinical and clinical studies,
853 and meta-analysis of determinants of antibody response variability af-
854 ter vaccination, *International Journal of Infectious Diseases* 74 (2018)
855 83–96.
- 856 [9] N. Venkatraman, D. Silman, P. M. Folegatti, A. V. Hill, Vaccines against
857 ebola virus, *Vaccine* 36 (36) (2018) 5454–5459.
- 858 [10] Eurosurveillance editorial team, First innovative medicines initiative
859 ebola projects launched, *Eurosurveillance* 20 (3) (2015) 21014.
- 860 [11] I. D. Milligan, M. M. Gibani, R. Sewell, E. A. Clutterbuck, D. Campbell,
861 E. Pledsted, E. Nuthall, M. Voysey, L. Silva-Reyes, M. J. McElrath, et al.,
862 Safety and immunogenicity of novel adenovirus type 26–and modified
863 vaccinia ankara–vectored ebola vaccines: a randomized clinical trial,
864 *Jama* 315 (15) (2016) 1610–1623.

- 865 [12] R. L. Winslow, I. D. Milligan, M. Voysey, K. Luhn, G. Shukarev,
866 M. Douoguih, M. D. Snape, Immune responses to novel adenovirus type
867 26 and modified vaccinia virus ankara–vectored ebola vaccines at 1 year,
868 *Jama* 317 (10) (2017) 1075–1077.
- 869 [13] G. Mutua, O. Anzala, K. Luhn, C. Robinson, V. Bockstal, D. Anu-
870 mendem, M. Douoguih, Safety and immunogenicity of a 2-dose heterol-
871 ogous vaccine regimen with Ad26. ZEBOV and MVA-BN-Filo Ebola
872 vaccines: 12-month data from a phase 1 randomized clinical trial in
873 Nairobi, Kenya, *The Journal of infectious diseases* 220 (1) (2019) 57–67.
- 874 [14] Z. Anywaine, H. Whitworth, P. Kaleebu, G. Praygod, G. Shukarev,
875 D. Manno, S. Kapiga, H. Grosskurth, S. Kalluvya, V. Bockstal, et al.,
876 Safety and immunogenicity of a 2-dose heterologous vaccination regimen
877 with Ad26. ZEBOV and MVA-BN-Filo Ebola vaccines: 12-month data
878 from a phase 1 randomized clinical trial in Uganda and Tanzania, *The*
879 *Journal of Infectious Diseases* 220 (1) (2019) 46–56.
- 880 [15] N. J. Sullivan, J. E. Martin, B. S. Graham, G. J. Nabel, Correlates
881 of protective immunity for ebola vaccines: implications for regulatory
882 approval by the animal rule, *Nature Reviews Microbiology* 7 (5) (2009)
883 393.
- 884 [16] G. Wong, J. S. Richardson, S. Pillet, A. Patel, X. Qiu, J. Alimonti,
885 J. Hogan, Y. Zhang, A. Takada, H. Feldmann, et al., Immune param-
886 eters correlate with protection against ebola virus infection in rodents
887 and nonhuman primates, *Science translational medicine* 4 (158) (2012)
888 158ra146–158ra146.
- 889 [17] J. M. Dye, A. S. Herbert, A. I. Kuehne, J. F. Barth, M. A. Muham-
890 mad, S. E. Zak, R. A. Ortiz, L. I. Prugar, W. D. Pratt, Postexposure
891 antibody prophylaxis protects nonhuman primates from filovirus dis-
892 ease, *Proceedings of the National Academy of Sciences* 109 (13) (2012)
893 5034–5039.
- 894 [18] B. Callendret, J. Vellinga, K. Wunderlich, A. Rodriguez, R. Steigerwald,
895 U. Dirmeier, C. Cheminay, A. Volkmann, T. Brasel, R. Carrion, et al., A
896 prophylactic multivalent vaccine against different filovirus species is im-
897 munogenic and provides protection from lethal infections with ebolavirus

- 898 and marburgvirus species in non-human primates, *PloS one* 13 (2) (2018)
899 e0192312.
- 900 [19] B. Pulendran, R. Ahmed, Translating innate immunity into immunolog-
901 ical memory: implications for vaccine development, *Cell* 124 (4) (2006)
902 849–863.
- 903 [20] L. Hviid, L. Barfod, F. J. Fowkes, Trying to remember: immunological
904 B cell memory to malaria, *Trends in parasitology* 31 (3) (2015) 89–94.
- 905 [21] D. L. Farber, M. G. Netea, A. Radbruch, K. Rajewsky, R. M. Zinker-
906 nagel, Immunological memory: lessons from the past and a look to the
907 future, *Nature Reviews Immunology* 16 (2) (2016) 124.
- 908 [22] T. Inoue, I. Moran, R. Shinnakasu, T. G. Phan, T. Kurosaki, Generation
909 of memory B cells and their reactivation, *Immunological reviews* 283 (1)
910 (2018) 138–149.
- 911 [23] G. D. Victora, M. C. Nussenzweig, Germinal centers, *Annual review of*
912 *immunology* 30 (2012) 429–457.
- 913 [24] N. S. De Silva, U. Klein, Dynamics of B cells in germinal centres, *Nature*
914 *reviews immunology* 15 (3) (2015) 137.
- 915 [25] M. J. Carter, R. M. Mitchell, P. M. Meyer Sauteur, D. F. Kelly, J. Trück,
916 The antibody-secreting cell response to infection: Kinetics and clinical
917 applications, *Frontiers in immunology* 8 (2017) 630.
- 918 [26] J. L. Halliley, S. Kyu, J. J. Kobie, E. E. Walsh, A. R. Falsey, T. D.
919 Randall, J. Treanor, C. Feng, I. Sanz, F. E.-H. Lee, Peak frequencies
920 of circulating human influenza-specific antibody secreting cells corre-
921 late with serum antibody response after immunization, *Vaccine* 28 (20)
922 (2010) 3582–3587.
- 923 [27] S. Leach, A. Lundgren, A.-M. Svennerholm, Different kinetics of circu-
924 lating antibody-secreting cell responses after primary and booster oral
925 immunizations: a tool for assessing immunological memory, *Vaccine*
926 31 (30) (2013) 3035–3038.
- 927 [28] A. A. Ademokun, D. Dunn-Walters, Immune responses: primary and
928 secondary, *Encyclopedia of Life Sciences*.

- 929 [29] S. G. Tangye, D. T. Avery, E. K. Deenick, P. D. Hodgkin, Intrinsic
930 differences in the proliferation of naive and memory human B cells as a
931 mechanism for enhanced secondary immune responses, *The Journal of*
932 *Immunology* 170 (2) (2003) 686–694.
- 933 [30] M. J. Shlomchik, Do memory B cells form secondary germinal centers?
934 yes and no, *Cold Spring Harbor perspectives in biology* 10 (1) (2018)
935 a029405.
- 936 [31] J. L. Halliley, C. M. Tipton, J. Liesveld, A. F. Rosenberg, J. Darce, I. V.
937 Gregoret, L. Popova, D. Kaminiski, C. F. Fucile, I. Albizua, et al.,
938 Long-lived plasma cells are contained within the cd19- cd38hicd138+
939 subset in human bone marrow, *Immunity* 43 (1) (2015) 132–145.
- 940 [32] E. Hammarlund, A. Thomas, I. J. Amanna, L. A. Holden, O. D. Slayden,
941 B. Park, L. Gao, M. K. Slifka, Plasma cell survival in the absence of B
942 cell memory, *Nature communications* 8 (1) (2017) 1781.
- 943 [33] F. Nommensen, S. Go, D. MacLaren, Half-life of hbs antibody after
944 hepatitis b vaccination: an aid to timing of booster vaccination, *The*
945 *Lancet* 334 (8667) (1989) 847–849.
- 946 [34] K. Van Herck, P. Van Damme, Inactivated hepatitis a vaccine-induced
947 antibodies: follow-up and estimates of long-term persistence, *Journal of*
948 *medical virology* 63 (1) (2001) 1–7.
- 949 [35] I. Van Twillert, A. A. B. Marinović, B. Kuipers, E. A. Sanders, C. A. van
950 Els, et al., Impact of age and vaccination history on long-term serological
951 responses after symptomatic b. pertussis infection, a high dimensional
952 data analysis, *Scientific Reports* 7 (2017) 40328.
- 953 [36] M. B. van Ravenhorst, A. B. Marinovic, F. R. van der Klis, D. M. van
954 Rooijen, M. van Maurik, S. P. Stoof, E. A. Sanders, G. A. Berbers, Long-
955 term persistence of protective antibodies in dutch adolescents following a
956 meningococcal serogroup c tetanus booster vaccination, *Vaccine* 34 (50)
957 (2016) 6309–6315.
- 958 [37] P. Teunis, O. Van Der Heijden, H. De Melker, J. Schellekens, F. Ver-
959 steegh, M. Kretzschmar, Kinetics of the igg antibody response to per-
960 tussis toxin after infection with b. pertussis, *Epidemiology & Infection*
961 129 (3) (2002) 479–489.

- 962 [38] D. Le, J. D. Miller, V. V. Ganusov, Mathematical modeling provides
963 kinetic details of the human immune response to vaccination, *Frontiers*
964 *in cellular and infection microbiology* 4 (2015) 177.
- 965 [39] R. J. De Boer, M. Oprea, R. Antia, R. Ahmed, A. S. Perelson, K. Murali-
966 krishna, Recruitment Times, Proliferation, and Apoptosis Rates during
967 the CD8⁺ T-cell Response to Lymphocytic Choriomeningitis Virus, *J.*
968 *Virol.* doi:10.1128/JVI.75.22.10663.
- 969 [40] R. Antia, C. T. Bergstrom, S. S. Pilyugin, S. M. Kaech, R. Ahmed,
970 [Models of CD8+ Responses: 1. What is the Antigen-independent](#)
971 [Proliferation Program](#), *J. Theor. Biol.* 221 (4) (2003) 585–598.
972 doi:10.1006/jtbi.2003.3208.
973 URL [http://linkinghub.elsevier.com/retrieve/pii/](http://linkinghub.elsevier.com/retrieve/pii/S0022519303932085)
974 [S0022519303932085](http://linkinghub.elsevier.com/retrieve/pii/S0022519303932085)
- 975 [41] C. Fraser, J. E. Tomassini, L. Xi, G. Golm, M. Watson, A. R. Giuliano,
976 E. Barr, K. A. Ault, Modeling the long-term antibody response of a hu-
977 man papillomavirus (hpv) virus-like particle (vlp) type 16 prophylactic
978 vaccine, *Vaccine* 25 (21) (2007) 4324–4333.
- 979 [42] M. Andraud, O. Lejeune, J. Z. Musoro, B. Ogunjimi, P. Beutels,
980 N. Hens, Living on three time scales: the dynamics of plasma cell and
981 antibody populations illustrated for hepatitis a virus, *PLoS Comput Biol*
982 8 (3) (2012) e1002418.
- 983 [43] M. T. White, J. T. Griffin, O. Akpogheneta, D. J. Conway, K. A. Ko-
984 ram, E. M. Riley, A. C. Ghani, Dynamics of the antibody response
985 to plasmodium falciparum infection in african children, *The Journal of*
986 *infectious diseases* 210 (7) (2014) 1115–1122.
- 987 [44] J. N. Wilson, D. J. Nokes, Do we need 3 doses of hepatitis b vaccine?,
988 *Vaccine* 17 (20) (1999) 2667–2673.
- 989 [45] J. N. Wilson, D. J. Nokes, G. F. Medley, D. Shouval, Mathematical
990 model of the antibody response to hepatitis b vaccines: implications for
991 reduced schedules, *Vaccine* 25 (18) (2007) 3705–3712.
- 992 [46] C. L. Davis, R. Wahid, F. R. Toapanta, J. K. Simon, M. B. Szein,
993 A clinically parameterized mathematical model of shigella immunity to
994 inform vaccine design, *PloS one* 13 (1) (2018) e0189571.

- 995 [47] C. Pasin, I. Balelli, T. Van Effelterre, V. Bockstal, L. Solfrosi,
996 M. Prague, M. Douoguih, R. Thiébaud, [Dynamics of the humoral](#)
997 [immune response to a prime-boost ebola vaccine: quantification and](#)
998 [sources of variation](#), *Journal of Virology* doi:10.1128/JVI.00579-19.
999 URL [https://jvi.asm.org/content/early/2019/06/20/JVI.](https://jvi.asm.org/content/early/2019/06/20/JVI.00579-19)
1000 [00579-19](#)
- 1001 [48] D. D. Jones, J. R. Wilmore, D. Allman, Cellular dynamics of memory
1002 B cell populations: IgM+ and IgG+ memory B cells persist indefinitely
1003 as quiescent cells, *The Journal of Immunology* (2015) 1501365.
- 1004 [49] S. Crotty, P. Felgner, H. Davies, J. Glidewell, L. Villarreal, R. Ahmed,
1005 Cutting edge: long-term B cell memory in humans after smallpox vac-
1006 cination, *The Journal of Immunology* 171 (10) (2003) 4969–4973.
- 1007 [50] P. Hartman, C. Olech, On global asymptotic stability of solutions of dif-
1008 ferential equations, *Transactions of the American Mathematical Society*
1009 104 (1) (1962) 154–178.
- 1010 [51] H. Miao, X. Xia, A. S. Perelson, H. Wu, On identifiability of nonlinear
1011 ode models and applications in viral dynamics, *SIAM review* 53 (1)
1012 (2011) 3–39.
- 1013 [52] H. B. Shah, K. A. Koelsch, B-cell elispot: for the identification of
1014 antigen-specific antibody-secreting cells, in: *Western Blotting*, Springer,
1015 2015, pp. 419–426.
- 1016 [53] M. Lavielle, L. Aarons, What do we mean by identifiability in mixed
1017 effects models?, *Journal of pharmacokinetics and pharmacodynamics*
1018 43 (1) (2016) 111–122.
- 1019 [54] J. Guedj, R. Thiébaud, D. Commenges, Maximum likelihood estimation
1020 in dynamical models of hiv, *Biometrics* 63 (4) (2007) 1198–1206.
- 1021 [55] M. Prague, D. Commenges, J. Guedj, J. Drylewicz, R. Thiébaud, Nim-
1022 rod: A program for inference via a normal approximation of the posterior
1023 in models with random effects based on ordinary differential equations,
1024 *Computer methods and programs in biomedicine* 111 (2) (2013) 447–
1025 458.

- 1026 [56] F. Sallusto, A. Lanzavecchia, K. Araki, R. Ahmed, From vaccines to
1027 memory and back, *Immunity* 33 (4) (2010) 451–463.
- 1028 [57] W. Jilg, M. Schmidt, F. Deinhardt, Vaccination against hepatitis b:
1029 comparison of three different vaccination schedules, *Journal of Infectious*
1030 *Diseases* 160 (5) (1989) 766–769.
- 1031 [58] R. B. Belshe, S. E. Frey, I. Graham, M. J. Mulligan, S. Edupuganti,
1032 L. A. Jackson, A. Wald, G. Poland, R. Jacobson, H. L. Keyserling,
1033 et al., Safety and immunogenicity of influenza a h5 subunit vaccines:
1034 effect of vaccine schedule and antigenic variant, *Journal of Infectious*
1035 *Diseases* 203 (5) (2011) 666–673.
- 1036 [59] R. L. Sheets, J. Stein, R. T. Bailer, R. A. Koup, C. Andrews, M. Nason,
1037 B. He, E. Koo, H. Trotter, C. Duffy, et al., Biodistribution and toxico-
1038 logical safety of adenovirus type 5 and type 35 vectored vaccines against
1039 human immunodeficiency virus-1 (hiv-1), ebola, or marburg are similar
1040 despite differing adenovirus serotype vector, manufacturer’s construct,
1041 or gene inserts, *Journal of immunotoxicology* 5 (3) (2008) 315–335.
- 1042 [60] T. Hanke, A. J. McMichael, M. J. Dennis, S. A. Sharpe, L. A. Powell,
1043 L. McLoughlin, S. J. Crome, Biodistribution and persistence of an mva-
1044 vectored candidate hiv vaccine in siv-infected rhesus macaques and scid
1045 mice, *Vaccine* 23 (12) (2005) 1507–1514.
- 1046 [61] Z. Zi, Sensitivity analysis approaches applied to systems biology models,
1047 *IET systems biology* 5 (6) (2011) 336–346.
- 1048 [62] G.-M. Li, C. Chiu, J. Wrammert, M. McCausland, S. F. Andrews, N.-
1049 Y. Zheng, J.-H. Lee, M. Huang, X. Qu, S. Edupuganti, et al., Pan-
1050 demic h1n1 influenza vaccine induces a recall response in humans that
1051 favors broadly cross-reactive memory b cells, *Proceedings of the National*
1052 *Academy of Sciences* 109 (23) (2012) 9047–9052.
- 1053 [63] J. Lessler, S. Riley, J. M. Read, S. Wang, H. Zhu, G. J. Smith, Y. Guan,
1054 C. Q. Jiang, D. A. Cummings, Evidence for antigenic seniority in in-
1055 fluenza a (h3n2) antibody responses in southern china, *PLoS pathogens*
1056 8 (7).
- 1057 [64] C. Green, C. Sande, C. De Lara, A. Thompson, L. Silva-Reyes,
1058 F. Napolitano, A. Pierantoni, S. Capone, A. Vitelli, P. Klenerman, et al.,

- 1059 Humoral and cellular immunity to rsv in infants, children and adults,
1060 Vaccine 36 (41) (2018) 6183–6190.
- 1061 [65] Ebovac2, 7th Ebovac2 e-newsletter, [http://www.ebovac2.com/
1062 images/EBOVAC2_newsletter7_19112018.pdf](http://www.ebovac2.com/images/EBOVAC2_newsletter7_19112018.pdf), Last accessed on 2020-
1063 01-31 (2018).
- 1064 [66] J. Karlsson, M. Anguelova, M. Jirstrand, An efficient method for struc-
1065 tural identifiability analysis of large dynamic systems, IFAC Proceedings
1066 Volumes 45 (16) (2012) 941–946.
- 1067 [67] A. Sedoglavic, A probabilistic algorithm to test local algebraic observ-
1068 ability in polynomial time, in: Proceedings of the 2001 international
1069 symposium on Symbolic and algebraic computation, ACM, 2001, pp.
1070 309–317.
- 1071 [68] H. Pohjanpalo, System identifiability based on the power series expan-
1072 sion of the solution, Mathematical biosciences 41 (1-2) (1978) 21–33.
- 1073 [69] Victor M. Garcia-Molla, Sensitivity analysis for odes and daes,
1074 MATLAB Central File Exchange, [https://fr.mathworks.com/
1075 matlabcentral/fileexchange/1480-sensitivity-analysis-for-
1076 odes-and-daes](https://fr.mathworks.com/matlabcentral/fileexchange/1480-sensitivity-analysis-for-odes-and-daes), Retrieved on 2017-09-07 (2017).
- 1077 [70] H. G. Bock, Numerical treatment of inverse problems in chemical re-
1078 action kinetics, in: Modelling of chemical reaction systems, Springer,
1079 1981, pp. 102–125.

1080 Appendix

1081 Appendix A. The IdentifiabilityAnalysis package

1082 In order to assess the *a priori* local structural identifiability of (MSL) we
1083 use the Exact Arithmetic Rank (EAR) approach implemented in Mathemat-
1084 ica through the IdentifiabilityAnalysis package [66]. It is the Mathe-
1085 matica implementation of a probabilistic semi-numerical algorithm described
1086 in [67] based on rank computation of a numerically instantiated Jacobian ma-
1087 trix. This is called the rank test for structural identifiability [68].

1088 **Appendix B. Matlab function `sens_ind` for numerical evaluation of**
1089 **partial derivatives**

1090 To evaluate the first-order partial derivatives of model outputs with re-
1091 spect to its parameters around a local point in the parameter space, we use
1092 Matlab function `sens_ind` [69]. It is based on Matlab function `ode15` and
1093 is able to compute the derivatives of an ODE system with respect to its
1094 parameters, by using the *Internal Numerical Differentiation* approach [70].

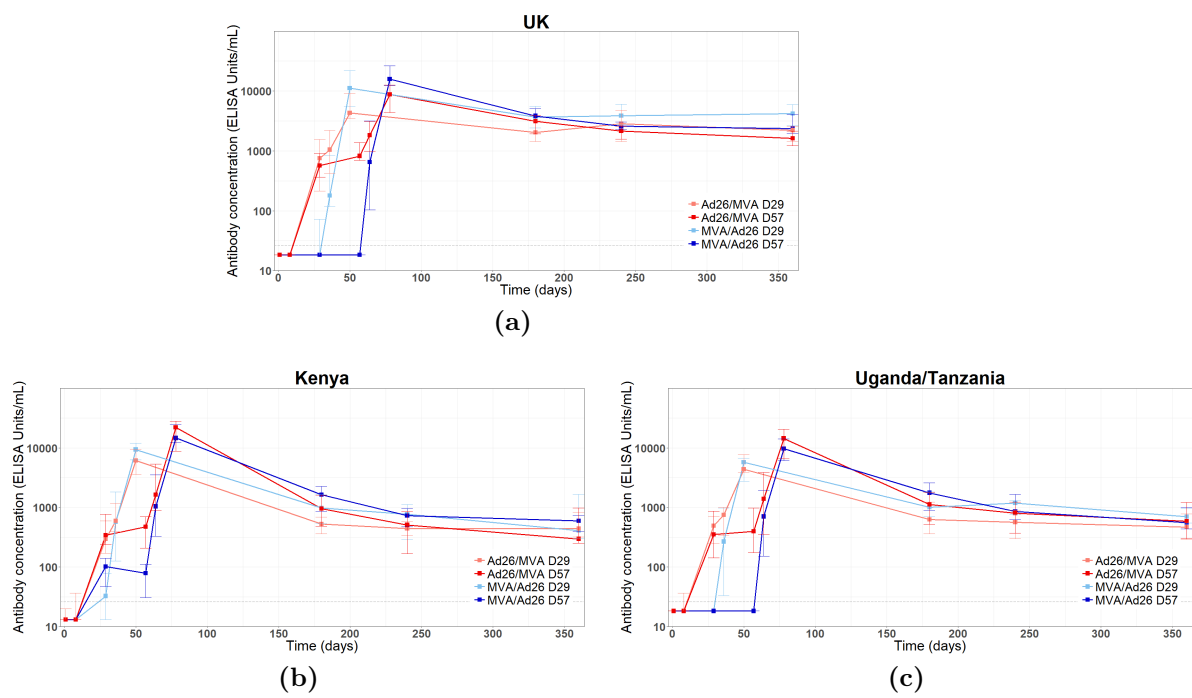


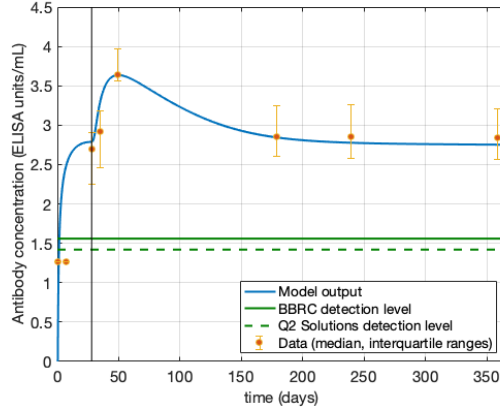
Figure S1: Antibody concentrations dynamics per site and vaccination groups in log₁₀ scale [47]. Medians and interquartile ranges are given.

Table S1: Summary of data in all studies.

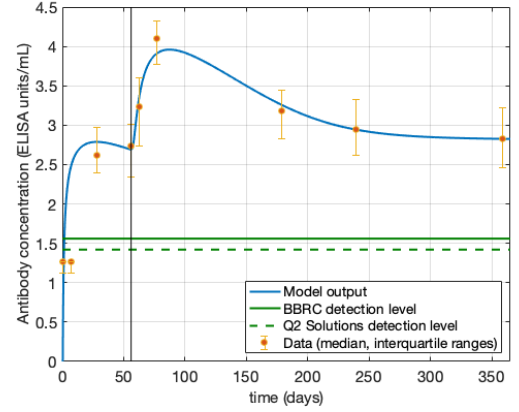
	UK	Kenya	Uganda/ Tanzania	Total
Number of participants, No.	59	59	59	177
Group MVA/Ad26 D29	15	14 (1 un- completed)	15	44
Group MVA/Ad26 D57	15	15	14 (1 un- completed)	44
Group Ad26/MVA D29	15	15	15	45
Group Ad26/MVA D57	14 (1 lost of follow-up)	15	15	44
Antibody concentrations (log₁₀ ELISA Units/mL), Mean (sd)	Detection level: 1.56	Detection level: 1.42	Detection level: 1.56	
Second dose injection day (first dose: Ad26.ZEBOV)	2.83 (0.5)	2.55 (0.44)	2.56 (0.43)	2.64 (0.47)
Second dose injection day (first dose: MVA-BN- Filo)	1.46 (0.36)	1.69 (0.48)	1.45 (0.46)	1.54 (0.44)
360 days post first dose (Ad26/MVA regimen)	3.24 (0.41)	2.63 (0.44)	2.74 (0.45)	2.85 (0.5)
360 days post first dose (MVA/Ad26 regimen)	3.51 (0.35)	2.77 (0.4)	2.84 (0.32)	3.03 (0.48)

Table S2: Details of the identifiability analysis results performed with `IdentifiabilityAnalysis` package (Section 4) for the (MSL) model. One can obtain the corresponding results for the reduced model (6) by supposing a_0 known. **DoF** = Degree of Freedom.

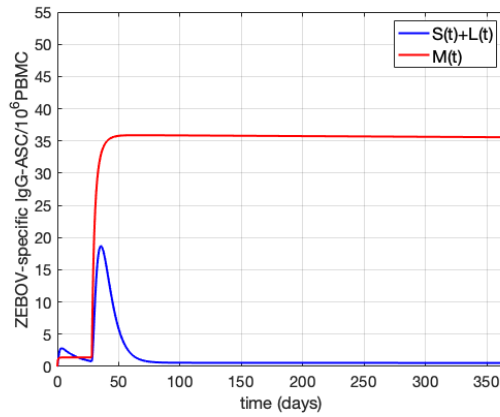
Input	Available outputs	Identifiability	DoF	Non-identifiable parameters
$\text{sys} = \{a'[t] = -da * a[t],$ $m'[t] = r * a[t] - (ms + ml) * a[t] * m[t] - dm * m[t],$ $s'[t] = ms * a[t] * m[t] - ds * s[t],$ $l'[t] = ml * a[t] * m[t] - dl * l[t],$ $Ab'[t] = ts * s[t] + tl * l[t] - dAb * Ab[t],$ $a[0] = a_0, m[0] = m_0, s[0] = s_0,$ $l[0] = l_0, Ab[0] = Ab_0\};$ $\text{states} = \{a, m, s, l, Ab\}$ $\text{params} = \{da, r, ms, ml, dm, ds, dl, ts, tl, db, a_0, m_0,$ $s_0, l_0, Ab_0\};$	$Ab_0, Ab[t]$	False	3	$a_0, m_0, s_0, l_0, r,$ ms, ml, tl, ts
	$Ab_0, Ab[t],$ ml, ms, r	True		
	$Ab_0, Ab[t],$ ml, ms, tl	True		
	$Ab_0, Ab[t],$ ml, ms, ts	True		
	$Ab_0, Ab[t],$ ml, r, ts	True		
	$Ab_0, Ab[t],$ ml, r, tl	True		
	$Ab_0, Ab[t],$ ml, tl, ts	True		
	$Ab_0, Ab[t],$ ms, r, ts	True		
	$Ab_0, Ab[t],$ ms, r, tl	True		
	$Ab_0, Ab[t],$ ms, tl, ts	True		
	$Ab_0, Ab[t],$ $s[t] + l[t]$	False	1	a_0, ml, ms, r
	$Ab_0, Ab[t],$ $s[t] + l[t], a_0$	True		
	$Ab_0, Ab[t],$ $m[t]$	False	2	$a_0, l_0, ml, ms, r, s_0,$ tl, ts



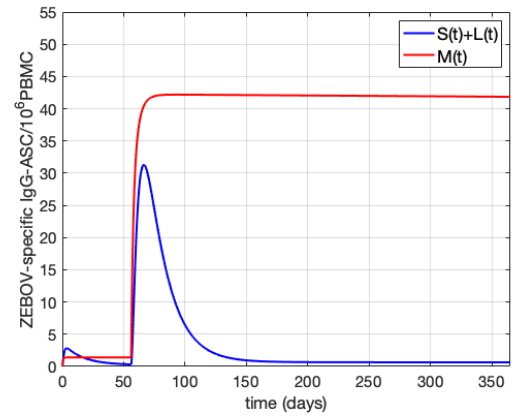
(a) $Ab(t)$, Ad26/MVA D29



(b) $Ab(t)$, Ad26/MVA D57

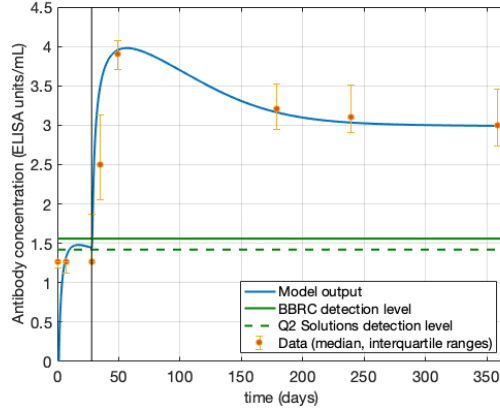


(c) B cells, Ad26/MVA D29

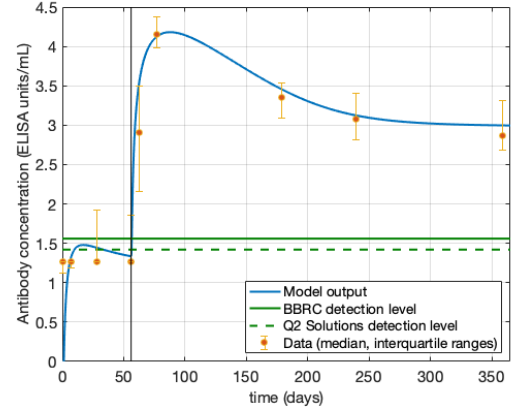


(d) B cells, Ad26/MVA D57

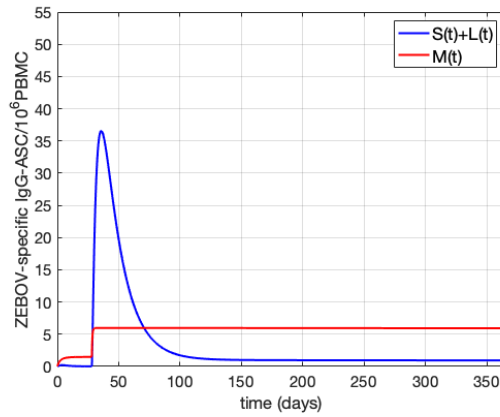
Figure S2: Results of the calibration of (6) (Section 5) for groups Ad26/MVA D29 (left column) and Ad26/MVA D57 (right column). In (a-b) green horizontal lines denote detection levels used by the BBRC laboratory (solid line) and by the Q2 Solutions laboratory (dashed line) respectively. Antibodies are \log_{10} -transformed.



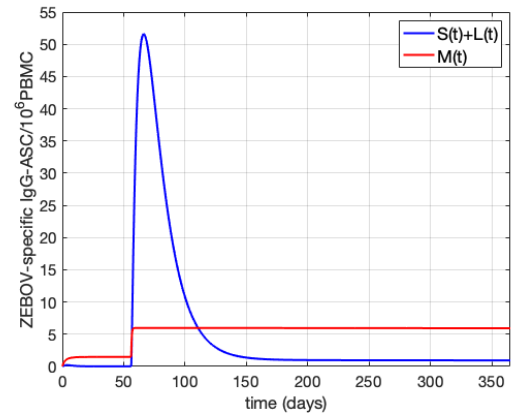
(a) $Ab(t)$, MVA/Ad26 D29



(b) $Ab(t)$, MVA/Ad26 D57



(c) B cells, MVA/Ad26 D29



(d) B cells, MVA/Ad26 D57

Figure S3: Results of the calibration of (6) (Section 5) for groups MVA/Ad26 D29 (left column) and MVA/Ad26 D57 (right column). In (a-b) green horizontal lines denote detection levels used by the BBRC laboratory (solid line) and by the Q2 Solutions laboratory (dashed line) respectively. Antibodies are \log_{10} -transformed.

Table S3: Antibody concentrations (in linear scale) obtained by model calibration for all vaccination groups, at some time points: the day of the second immunization (2D day), 21 days after the second dose (P2D) and 360 days after the first dose. We compare simulated values obtained with (6) with the parameter set detailed in Table 4 to data described in Section 2.

Group		2D day	21 days P2D	Day 360
Ad26/MVA D29	simulated value	613	4324	565
	data, median (iqr)	492 (625)	4349 (5768)	693 (1268)
Ad26/MVA D57	simulated value	489	8147	670
	data, median (iqr)	550 (797)	12468 (15151)	671 (1360)
MVA/Ad26 D29	simulated value	28	8954	981
	data, median (iqr)	18 (55)	8101 (6736)	1009 (2340)
MVA/Ad26 D57	simulated value	27	13354	994
	data, median (iqr)	18 (53)	14276 (14077)	740 (1556)

Table S4: Antibody concentrations (in linear scale) obtained by simulation of (6) with a booster Ad26.ZEBOV immunization realized 1 year after the first dose (day 360). We compare vaccination groups Ad26/MVA D29 and Ad26/MVA D57.

Immunization schedule	Day 360	Day 367	Day 381	Day 720
Ad26/MVA D29 + Ad26 D360	576	7054	16943	1647
Ad26/MVA D57 + Ad26 D360	683	7635	17584	1767